Electronic Supplementary Material (ESI) for Polymer Chemistry.

Supplementary Information

Towards Scalable, Low Dispersity, and Dimensionally Tunable 2D Platelets using Living Crystallization-Driven Self-Assembly

Charlotte E. Ellis,[a] Tomoya Fukui,[‡a] Cristina Cordoba,[b] Arthur Blackburn[b] and Ian Manners*[a]

[a] Department of Chemistry, University of Victoria, Victoria, BC V8P 5C2, Canada

[b] Department of Physics and Astronomy, University of Victoria, Victoria, BC V8P 5C2, Canada

[‡] Present address: Tokyo Institute of Technology, R1-1, 4259 Nagatsuta, Midori-ku, Yokohama, Kanagawa, 226-8503, Japan

*To whom correspondence should be addressed: imanners@uvic.ca

Materials

Solvents were dried and de-oxygenated using a Solvent Purification System (SPS). THF used for anionic polymerization was distilled from Na/benzophenone. All materials were purchased from Sigma-Aldrich and used as received unless otherwise stated. Self-assembly experiments were performed in HPLC grade solvents, filtered through a 0.2 μm membrane. Dimethylsila[1]ferrocenophane was prepared by literature procedure.[1] Polymers PFS_{24}-*b*-$P2VP_{384}$ (M_n = 46,420 Da, M_w/M_n = 1.19), $PFS_{23}[PPh_2Me]I$ (M_n = 5,830 Da, M_w/M_n = 1.07), and PFS_{20}-*b*-$P2VP_{19}$ (M_n = 6,450 Da, M_w/M_n = 1.10), were prepared by literature procedures.[2,3]

Material Characterisation

NMR spectroscopy

^1H and ^{31}P NMR were obtained using a Varian 500 MHz spectrometer. ^{13}P NMR analyses used an internal reference of triphenylphosphine in THF (100 mg/mL). ^1H DOSY NMR was conducted using a Varian 500 MHz spectrometer, with a 900 ms diffusion delay (Δ) and a diffusion gradient length (δ) of 2500 μs. Polymer and surfactant samples were analysed at a concentration of 5 mg/mL or 10 mg/mL, respectively. NMR data was processed using MestReNova.

Gel permeation chromatography (GPC)

GPC was conducted using a Malvern Omnisec Resolve/Reveal equipped with a triple detector array, automatic sampler, pump, injector, inline degasser column oven (set at 35 °C), elution columns consisting of styrene/divinylbenzene gels (of pore size 500–5,000 Å), refractometer, four-capillary differential viscometer, UV/Vis detector (λ = 440 nm) and dual angle laser light scattering

detector (7° and 90°). GPC grade THF with 1 wt% triethylamine was used as the eluent, with a set flow rate of 1 mL/min. Samples were dissolved in THF at 2 mg/mL and filtered through a 0.2 μm polytetrafluoroethylene membrane prior to analysis.

Matrix-assisted laser desorption/ionization time-of-flight (MALDI-TOF) mass spectrometry

MALDI-TOF was performed on a Bruker Ultraflex III TOF/TOF instrument. Samples were prepared by mixing 10 μL of polymer sample in THF (2 mg/mL) with 100 μL of trans-2-[3-(4-*tert*-butylphenyl)-2-methyl-2-propenylidene] malonitrile in THF (20 mg/mL). Approximately 2 μL of this mixture was deposited onto a polished steel plate and allowed to dry.

Transmission electron microscopy (TEM)

Copper grids (500 mesh) were purchased from Ted Pella, Inc. and carbon films were prepared by using a Leica EM ACE600 instrument. Carbon films were deposited onto the copper grids by floatation on water and allowed to dry over 24 hours. Samples for electron microscopy were prepared by drop-casting 8 μL of micelle colloidal solution onto a carbon-coated copper grid followed by solvent evaporation. TEM images were obtained using a JEOL JEM 1011 operating at 80 kV, equipped with a Gatan Orius SC1000 CCD camera.

Measurements were undertaken by hand using ImageJ software, developed by the US National Institute for Health. The platelet area (A), length (L) and width (W) were measured by using the rotated rectangle tool. The aspect ratio (R) was calculated for each platelet by the following equation:

$$R = \frac{L}{W}$$

The number-average area (A_n) and weight-average area (A_w) were calculated according to the following equations:

$$A_n = \frac{\sum_i^n N_i A_i}{\sum_i^n N_i} \qquad A_w = \frac{\sum_i^n N_i A_i^2}{\sum_i^n N_i A_i}$$

The number-average length (L_n) and weight-average length (L_w) were calculated according to the following equations:

$$L_n = \frac{\sum_i^n N_i L_i}{\sum_i^n N_i} \qquad L_w = \frac{\sum_i^n N_i L_i^2}{\sum_i^n N_i L_i}$$

The number-average width (W_n) and weight-average width (W_w) were calculated according to the following equations:

$$W_n = \frac{\sum_i^n N_i W_i}{\sum_i^n N_i} \qquad W_w = \frac{\sum_i^n N_i W_i^2}{\sum_i^n N_i W_i}$$

The number-average aspect ratio (R_n) and weight-average aspect ratio (R_w) were calculated according to the following equations:

$$R_n = \frac{\sum_i^n N_i R_i}{\sum_i^n N_i} \qquad R_w = \frac{\sum_i^n N_i R_i^2}{\sum_i^n N_i R_i}$$

A minimum of 100 micelles were measured for each data point. Errors displayed are standard deviations of each data set.

Selected-area electron diffraction (SAED) analysis

Four-dimensional scanning transmission electron microscopy (4D-STEM) data for 2D nanostructures was collected using a STEM Hitachi HF-3300v with a hybrid pixel array detector MerlinEM (Quantum Detectors) operating in low-magnification mode at 200 kV. Hitachi High-

Technologies Canada's Azorus software was used to control and acquire diffraction data. Diffraction data was collected from a 2.5 x 3.5 µm sample area on a 30 x 40 grid. In the surveyed area, 1,200 diffraction patterns were collected. The sample was exposed to the beam (beam size = 70 nm) for 2 ms during collection each diffraction pattern, giving an average dose of approximately 3 $e^-/Å^2$, including the preacquisition sample positioning exposure. Resulting data from such acquisitions was first inspected using Azorus software. Post-collection processing was performed using pixStem and HyperSpy open-source Python libraries from multidimensional data analysis. It should be noted that obtaining further evidence for the core crystallinity was challenging due to issues with the beam-sensitivity of the PFS-based platelets, as well as beam overlap with the central 1D PFS_{24}-*b*-$P2VP_{384}$ seed.

Dynamic light scattering (DLS)

DLS was performed using a Malvern Panalytical Zetasizer Ultra/Pro instrument equipped with a laser with a wavelength of 633 nm and a detector oriented at 173º to the incident radiation.

Ultrasonication

Micelle sonication was carried out using a Fisherbrand FB11203 sonication bath (37 W sonication power).

Synthesis of Materials

Synthesis of phosphine-terminated PFS homopolymer, $PFS_{23}PPh_2$

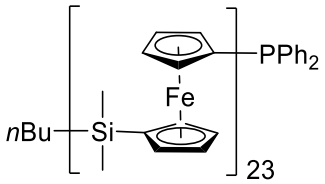

Dimethylsila[1]ferrocenophane (484 mg, 2.00 mmol) in dry, degassed tetrahydrofuran (THF) (5 mL) was initiated with *n*-butyl lithium (1.6 M in hexanes, 63 µL, 0.10 mmol) at room temperature to target a degree of polymerization (DP_n) of 20. After 45 min, the colour of the solution had changed from red to amber, indicating complete conversion of the monomer. The reaction was terminated by the addition of chlorodiphenylphosphine (373 µL, 2.02 mmol) and stirred for 90 min. The resulting polymer was precipitated into degassed methanol, followed by washing with the same non-solvent 3 times. The polymer was dried under vacuum for 1 h to afford an orange solid. ^{1}H NMR analysis was used to determine the homopolymer structure of $PFS_{23}PPh_2$.

Yield: 387 mg (80%). ^{1}H NMR (500 MHz, $CDCl_3$): δ (ppm) = 7.39–7.29 (m, 10H, P*Ph*$_2$), 4.21 (m, 92H, Cp*H*), 4.01 (m, 92H, Cp*H*), 0.46 (s, 138H, Si(C*H*$_3$)$_2$), 0.40 (s, 2H, Me(CH$_2$)$_2$C*H*$_2$SiMe$_2$), 0.19 (s, 6H, *n*-BuSi(C*H*$_3$)$_2$); ^{31}P NMR (500 MHz, $CDCl_3$): δ (ppm) = -17.5; M_w/M_n (GPC) = 1.08.

Quaternization of phosphine-terminated PFS homopolymer to prepare the phosphonium derivative $PFS_{23}[PPh_2Me]I$

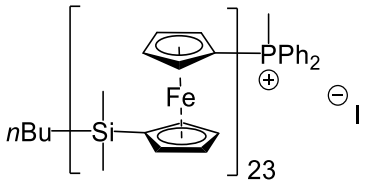

To a solution of $PFS_{23}PPh_2$ (300 mg, 0.06 mmol) in THF (3 mL) was added an excess of MeI (300 µL, 4.80 mmol). After 3 h, the polymer was precipitated in degassed hexanes, followed by washing with hexanes 3 times. The polymer was dried under vacuum for 1 h to afford an orange solid. Complete quaternization was determined using integration of the P*Ph*$_2$ (7.77–7.61 ppm) and P-C*H*$_3$ (3.04 ppm) proton resonances within the ^{1}H NMR spectrum (Figure S1a,b). The polymer was stored in the absence of light. Using the degree of polymerization (DP_n) determined via ^{1}H NMR analysis (DP_n = 23), the M_n could be calculated through summation of the molar masses of the *n*-butyl and phosphonium end groups with that of the main chain: (242.17 Da x 23) + 57.12 Da + 200.19 Da = 5827.22 Da. This value was in good agreement with the M_n obtained via MALDI-TOF mass spectrometry.

Yield: 278 mg (90%). ^{1}H NMR (500 MHz, $CDCl_3$): δ (ppm) = 7.77–7.61 (m, 10H, P*Ph*$_2$), 4.56 (t, 2H, Cp(α-*H*)-[$PPh_2Me]^+$) 4.36 (t, 2H, Cp(β-*H*)-[$PPh_2Me]^+$) 4.21 (m, 92H, Cp*H*), 4.01 (m, 92H, Cp*H*), 3.04 (d, J = 13.0 Hz, 3H, P-C*H*$_3$), 0.46 (s, 138H, Si(C*H*$_3$)$_2$), 0.34 (m, 6H, Si(C*H*$_3$)$_2$(Cp)Fe(Cp)-[$PPh_2Me]^+$), 0.19 (s, 6H, *n*-BuSi(C*H*$_3$)$_2$); ^{31}P NMR (500 MHz, THF): δ (ppm) = +24.1; M_n (MALDI-TOF) = 5,830 Da; M_n (^{1}H NMR) = 5,827 Da; M_w/M_n (GPC) = 1.07.

Anion exchange of $PFS_{23}[PPh_2Me]I$ homopolymer to prepare $PFS_{23}[PPh_2Me]SDS$

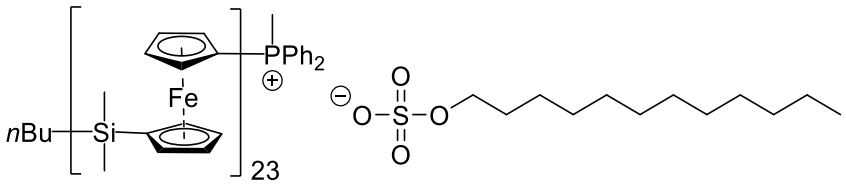

To a solution of $PFS_{23}[PPh_2Me]I$ (100 mg, 0.02 mmol) in THF (3 mL) was added an excess of sodium dodecyl sulfate, [SDS]Na, (952 mg, 3.30 mmol). A precipitate formed immediately. The reaction was stirred for 1 h before precipitation into methanol. The polymer was washed with

methanol 3 times to remove NaI. Drying under vacuum for 1 h afforded an orange solid. The polymer was stored in the absence of light. Complete anion exchange was confirmed by ^{1}H NMR through integration analysis of the ratio of the P*Ph*$_2$ and -C*H*$_2$- signals. Using the degree of polymerization (DP$_n$) determined via ^{1}H NMR analysis (DP$_n$ = 23), the M_n could be calculated through summation of the molar masses of the *n*-butyl and phosphonium end groups with that of the main chain: (242.17 Da x 23) + 57.12 Da + 200.19 Da = 5827.22 Da. This value was in good agreement with the M_n obtained via MALDI-TOF mass spectrometry.

Yield: 97 mg (92%). ^{1}H NMR (500 MHz, $CDCl_3$): δ (ppm) = 7.72–7.60 (m, 10H, P*Ph*$_2$), 4.55 (t, 2H, Cp(α-*H*)-[PPh$_2$Me]$^+$), 4.42 (t, 2H, Cp(β-*H*)-[PPh$_2$Me]$^+$), 4.21 (m, 92H, Cp*H*), 4.02 (m, 92H, Cp*H*), 2.97 (d, J = 13.0 Hz, 3H, P-C*H*$_3$), 2.22 (t, J = 7.0 Hz, 1H, (SO$_4$)C*H*$_2$-), 2.01 (d, 7.0 Hz, 1H, (SO$_4$)C*H*$_2$-), 1.68 (p, J = 7.0 Hz, 2H, (SO$_4$)CH$_2$C*H*$_2$-), 1.36–1.23 (m, 18H, -C*H*$_2$-), 0.46 (s, 138H, Si(C*H*$_3$)$_2$), 0.34 (m, 6H, Si(C*H*$_3$)$_2$(Cp)Fe(Cp)-[PPh$_2$Me]$^+$), 0.21 (s, 6H, *n*-BuSi(C*H*$_3$)$_2$); ^{31}P NMR (500 MHz, THF): δ (ppm) = +23.8; M_n (MALDI-TOF) = 5,830 Da; M_n (^{1}H NMR) = 5,827 Da; M_w/M_n (GPC) = 1.07.

Anion exchange of PFS$_{23}$[PPh$_2$Me]I homopolymer to prepare PFS$_{23}$[PPh$_2$Me]AOT

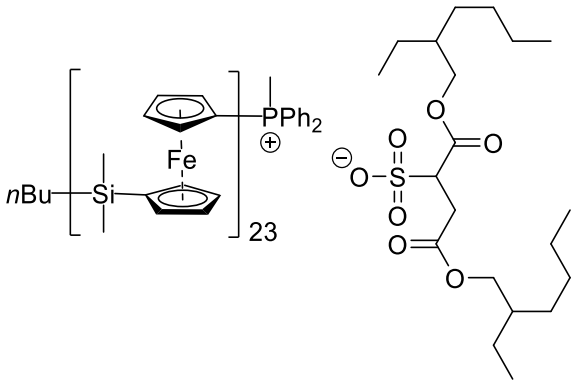

To a solution of PFS$_{23}$[PPh$_2$Me]I (100 mg, 0.02 mmol) in THF (3 mL) was added an excess of dioctyl sulfosuccinate sodium salt, [AOT]Na, (1.47 g, 3.30 mmol). A precipitate formed

immediately. The reaction was stirred for 1 h before precipitation into methanol. The polymer was washed with methanol 3 times to remove NaI. After drying under vacuum for 1 h, an orange solid was afforded. The polymer was stored in the absence of light. Complete anion exchange was confirmed by ^{1}H NMR through integration analysis of the ratio of the P*Ph*$_2$ and C*H*$_2$ signals. Using the degree of polymerization (DP_n) determined via ^{1}H NMR analysis (DP_n = 23), the M_n could be calculated through summation of the molar masses of the *n*-butyl and phosphonium end groups with that of the main chain: (242.17 Da x 23) + 57.12 Da + 200.19 Da = 5827.22 Da. This value was in good agreement with the M_n obtained via MALDI-TOF mass spectrometry.

Yield: 102 mg (94%). ^{1}H NMR (500 MHz, $CDCl_3$): δ (ppm) = 7.74–7.59 (m, 10H, P*Ph*$_2$), 4.52 (t, 2H, Cp(α-*H*)-[$PPh_2Me]^+$), 4.42 (t, 2H, Cp(β-*H*)-[$PPh_2Me]^+$), 4.21 (t, J = 2.0 Hz, 92H, Cp*H*), 4.01 (t, J = 2.0 Hz, 92H, Cp*H*), 3.97–3.90 (m, 4H, -C*H*$_2$COO-), 3.36 (dd, J = 17.5, 12.0 Hz, 1H, -CH(SO_3)C*H*$_2$-), 3.18 (dd, J = 17.5, 3.0 Hz, 1H, -CH(SO_3)C*H*$_2$-), 2.96 (d, J = 13.5 Hz, 3H, P-C*H*$_3$), 1.48–1.39 (m, 2H, -C*H*-), 1.37–1.27 (m, 16H, -C*H*$_2$-), 0.88–0.81 (m, 12H, -CH_2C*H*$_3$), 0.46 (s, 138H, Si(C*H*$_3$)$_2$), 0.31 (m, 6H, Si(C*H*$_3$)$_2$(Cp)Fe(Cp)-[$PPh_2Me]^+$), 0.19 (s, 6H, *n*-BuSi(C*H*$_3$)$_2$); ^{31}P NMR (500 MHz, THF): δ (ppm) = +23.6; M_n (MALDI-TOF) = 5,830 Da; M_n (^{1}H NMR) = 5,827 Da; M_w/M_n (GPC) = 1.07.

Synthesis of PFS$_{24}$-*b*-P2VP$_{384}$

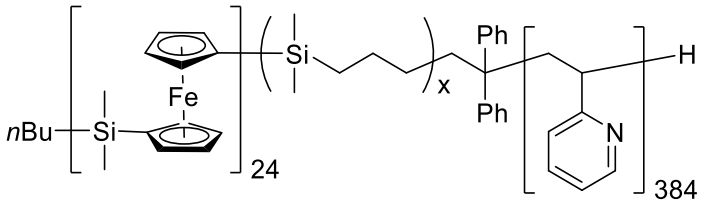

Dimethylsila[1]ferrocenophane (210 mg, 0.87 mmol) in THF (2 mL) was initiated with *n*-butyl lithium (1.6 M in hexanes, 22 µL, 0.04 mmol) at room temperature. After 30 min, the colour of

the solution changed from red to amber, indicating complete conversion of the monomer. Sequential addition of 1,1-dimethylsilacyclobutane (DMSB) (14 µL, 0.11 mmol) followed by 1,1-diphenylethylene (DPE) (37.0 µL, 0.21 mmol) into the living PFS polymer solution caused a change in colour from amber to dark red within a minute, indicating the formation of a diphenylmethyl-type carbanion. After a total of 40 min, an aliquot (415 µL) for molecular weight analysis was removed and quenched with 4-*t*-butylphenol. Dry LiCl (ca. 10 mg) and 2-vinylpyridine (1.2 mL, 11.1 mmol) were dissolved in THF (5.6 mL). The living PFS and 2-vinylpyridine/LiCl solutions were both cooled to -78 °C for 15 min before they were combined. The reaction proceeded for 60 min at -78 °C before termination with 4-*t*-butylphenol. The polymer was precipitated into hexanes from THF 3 times and was then dried under vacuum overnight to afford a light orange solid. GPC and ^{1}H NMR analysis were used to determine the final block copolymer composition of PFS_{24}-*b*-$P2VP_{384}$.

Yield: 1.06 g (77%). ^{1}H NMR (500 MHz, $CDCl_3$): δ (ppm) = 8.23 (m, 16H, NC*H*C), 7.26–6.16 (m, 48H, aromatic *H*), 4.21 (m, 4H, Cp*H*), 4.00 (m, 4H, Cp*H*), 2.40–1.42 (br, alkyl *H*), 0.45 (s, 6H, Si(CH_3)$_2$); M_n (GPC) = 46,420 Da; M_w/M_n (GPC) = 1.19.

Synthesis of PFS_{20}-*b*-$P2VP_{19}$

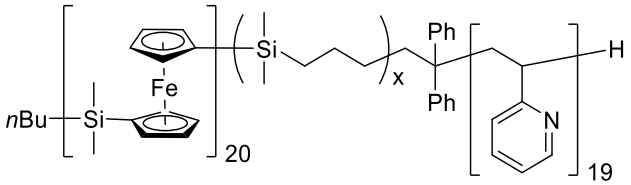

Dimethylsila[1]ferrocenophane (100 mg, 0.4 mmol) in THF (2 mL) was initiated with *n*-butyl lithium (1.6 M in hexanes, 10 µL, 0.016 mmol) at room temperature. After 30 min, the colour of the solution changed from red to amber, indicating complete conversion of the monomer. Sequential addition of 1,1-dimethylsilacyclobutane (DMSB) (6.2 µL, 0.048 mmol) followed by

1,1-diphenylethylene (DPE) (17 µL, 0.096 mmol) into the living PFS polymer solution caused a change in colour from amber to dark red within a minute, indicating the formation of a diphenylmethyl-type carbanion. After a total of 40 min, an aliquot (250 µL) for molecular weight analysis was removed and quenched with 4-*t*-butylphenol. Dry LiCl (ca. 1 mg) and 2-vinylpyridine (32 µL, 0.3 mmol) were dissolved in THF (500 µL). The living PFS and 2-vinylpyridine/LiCl solutions were both cooled to -78 °C for 15 min before they were combined. The reaction proceeded for 40 min at -78 °C before termination with 4-*t*-butylphenol. The polymer was precipitated into hexanes from THF 3 times and was then dried under vacuum overnight to afford a light orange solid. MALDI-TOF and ^{1}H NMR analysis were used to determine the final block copolymer composition of PFS_{20}-*b*-$P2VP_{19}$.

Yield: 89 mg (68%). ^{1}H NMR (500 MHz, $CDCl_3$): δ (ppm) = 8.22 (m, 1H, NC*H*C), 7.22–6.22 (m, 3H, aromatic *H*), 4.22 (s, 4H, Cp*H*), 4.02 (s, 4H, Cp*H*), 2.40–1.46 (br, alkyl *H*), 0.44 (s, 6H, $Si(CH_3)_2$); M_n (GPC) = 6,450 Da; M_w/M_n (GPC) = 1.10.

Self-Assembly

Formation of uniform 1D PFS_{24}-*b*-$P2VP_{384}$ cylindrical seed micelles (L_n = 26 nm, L_w/L_n = 1.19) at 0.6 wt%

A 5 mg/mL (0.6 wt%) solution of PFS_{24}-*b*-$P2VP_{384}$ in *i*PrOH was prepared and heated at 80 °C with stirring for 24 h, to ensure complete dissolution of the polymer. The solution was left to cool slowly to room temperature (22 ºC) without stirring after turning off the heating source. TEM analysis after a further 24 h confirmed the presence of polydisperse cylindrical micelles. The fibres were sonicated at 0 °C for 4 h, to yield low aspect ratio by polydisperse micelles (L_n = 22 ± 15 nm,

L_w/L_n = 1.46). These fibres were then annealed at 80 °C for 30 min to improve the micelle length dispersity. Uniform 1D seed micelles resulted and were carefully measured by hand using ImageJ software (as previously described on page S3). L_n = 26 ± 10 nm, L_w/L_n = 1.19.

Formation of uniform 2D platelet micelles at 0.01 wt%

To *i*PrOH (1 mL) was added 25 μL of PFS_{24}-*b*-$P2VP_{384}$ seeds (L_n = 26 nm, L_w/L_n = 1.19) in *i*PrOH (0.5 mg/mL). To this colloidal solution was added a specific amount of unimer solution in THF (10 mg/mL) whilst vigorously shaking by vortex mixer for 3 s. The solution was left for 24 h before TEM analysis. Uniform low-aspect ratio platelets were observed and were carefully measured by hand using ImageJ software (as described on page S3).

Formation of 2D platelet micelles at scalable concentrations (0.1–0.4 wt%)

To various amounts of iPrOH (to prepare 1, 2, 3, 4 and 5 mg/mL solutions) was added 10 μL of PFS_{24}-*b*-$P2VP_{384}$ seeds (L_n = 26 nm, L_w/L_n = 1.19) in *i*PrOH (5 mg/mL). The solution was manually shaken for 3 s before 50 μL of unimer solution in THF (10 mg/mL) was added whilst vigorously shaking by vortex mixer for 3 s. The solutions were left for 12 h before TEM analysis. Samples diluted to 0.1 mg/mL for analysis. The resultant nanostructures were carefully measured by hand using ImageJ software (as described on page S3).

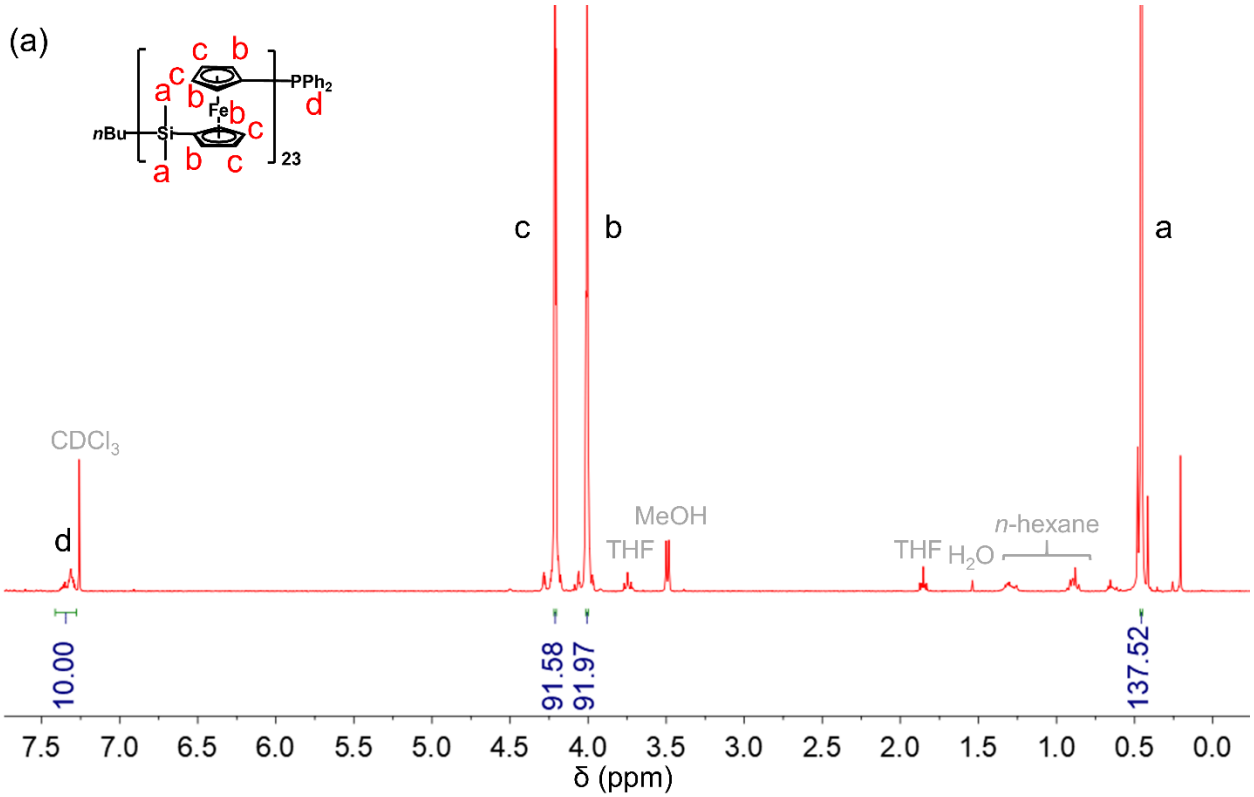
(a)
nBu
Si
Fe
PPh2
23
c
b
a
CDCl3
d
MeOH
THF
THF
H2O
n-hexane
10.00
91.58
91.97
137.52
7.5 7.0 6.5 6.0 5.5 5.0 4.5 4.0 3.5 3.0 2.5 2.0 1.5 1.0 0.5 0.0
δ (ppm)

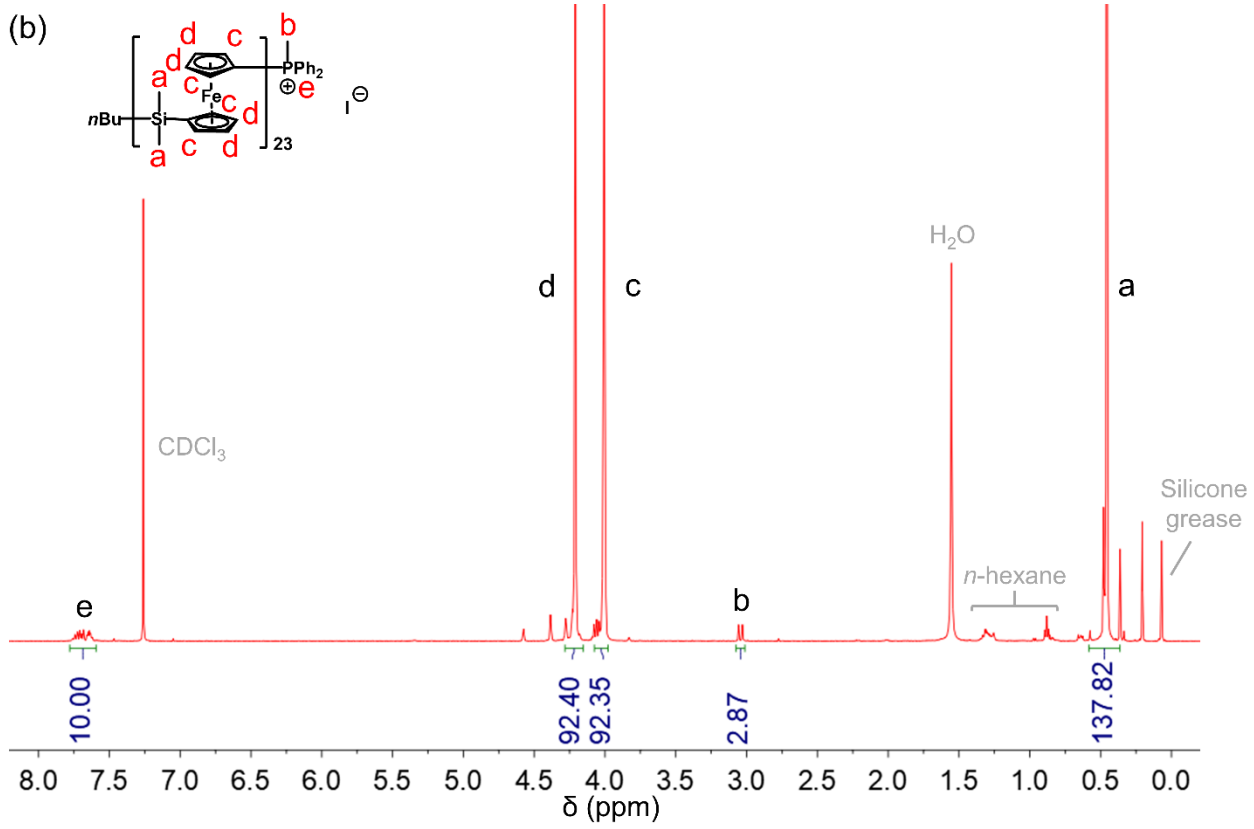
(b)
nBu
Si
Fe
PPh2
e
I⊖
23
d
c
b
a
CDCl3
H2O
n-hexane
Silicone grease
e
10.00
92.40
92.35
2.87
137.82
8.0 7.5 7.0 6.5 6.0 5.5 5.0 4.5 4.0 3.5 3.0 2.5 2.0 1.5 1.0 0.5 0.0
δ (ppm)

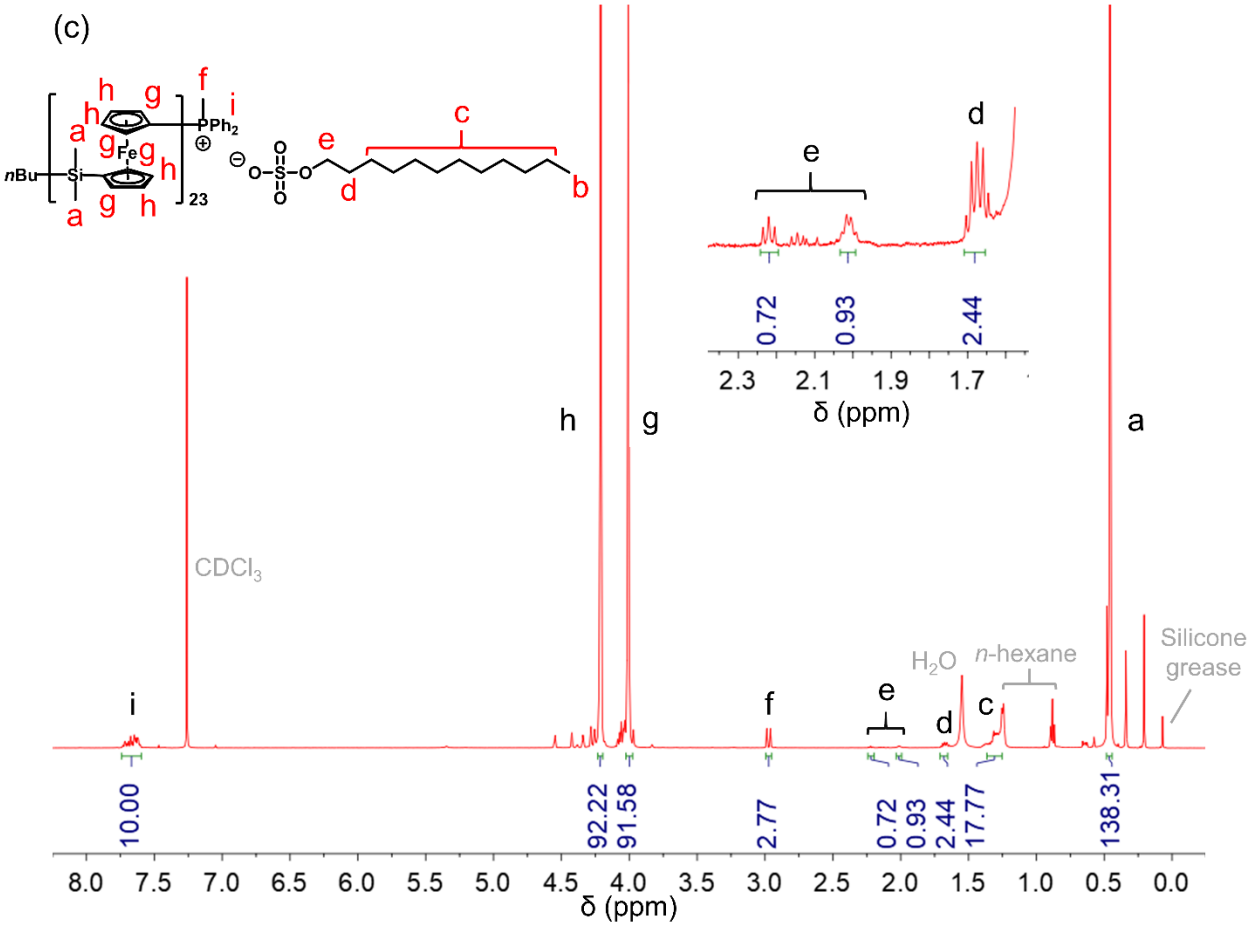
(c)
nBu
Si
Fe
PPh2
23
a
b
c
d
e
f
g
h
i
CDCl3
H2O
n-hexane
Silicone grease
10.00
92.22
91.58
2.77
0.72
0.93
2.44
17.77
138.31
0.72
0.93
2.44
δ (ppm)

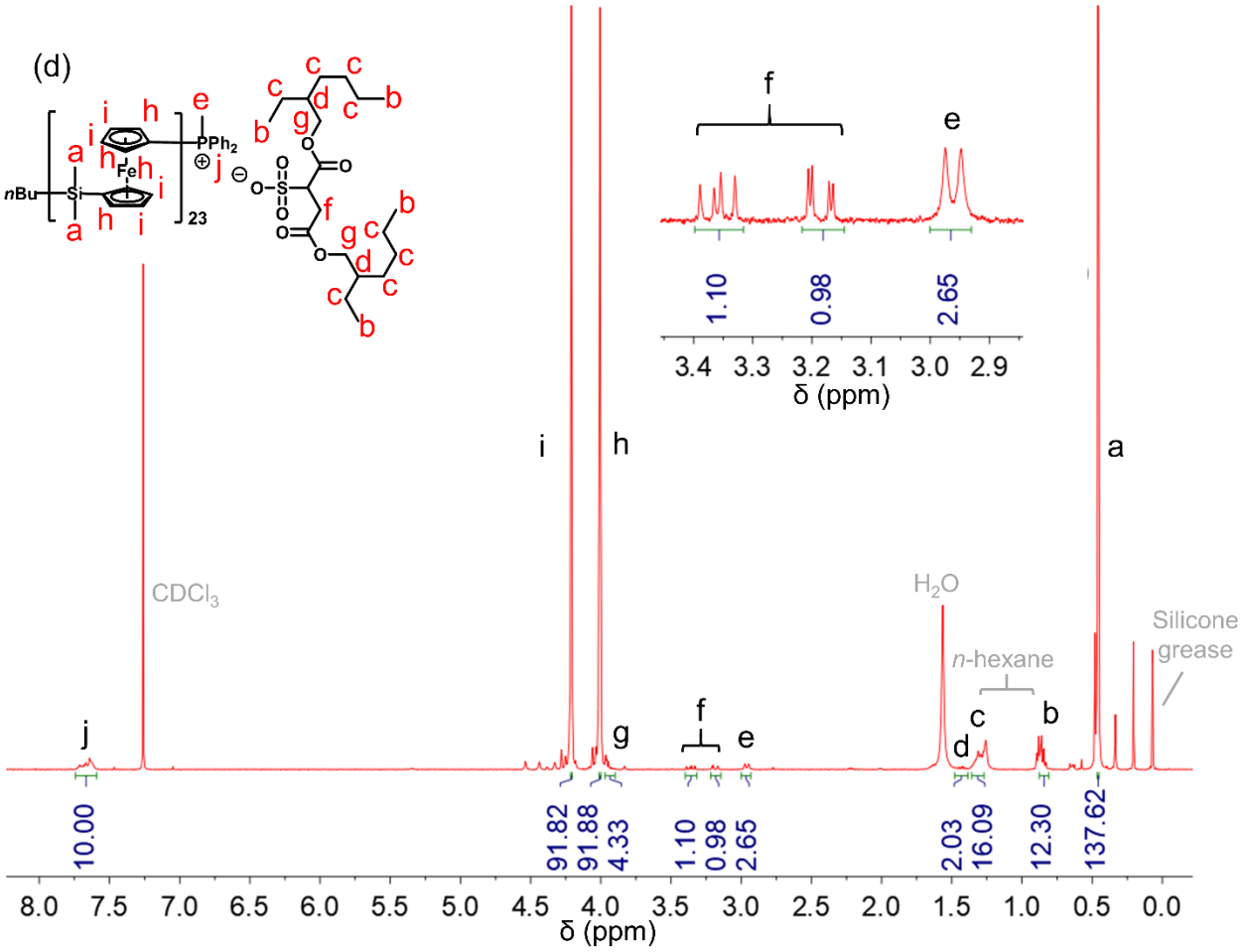

Fig. S1 ^{1}H NMR spectra (in $CDCl_3$) of (a) $PFS_{23}PPh_2$, compared with quaternized (b) $PFS_{23}[PPh_2Me]I$, (c) $PFS_{23}[PPh_2Me]SDS$ and (d) $PFS_{23}[PPh_2Me]AOT$. Small peaks at 4.56–4.36 ppm and 0.34–0.19 ppm correspond to locations near the polymer chain termini and are assigned on pages S6–S9.

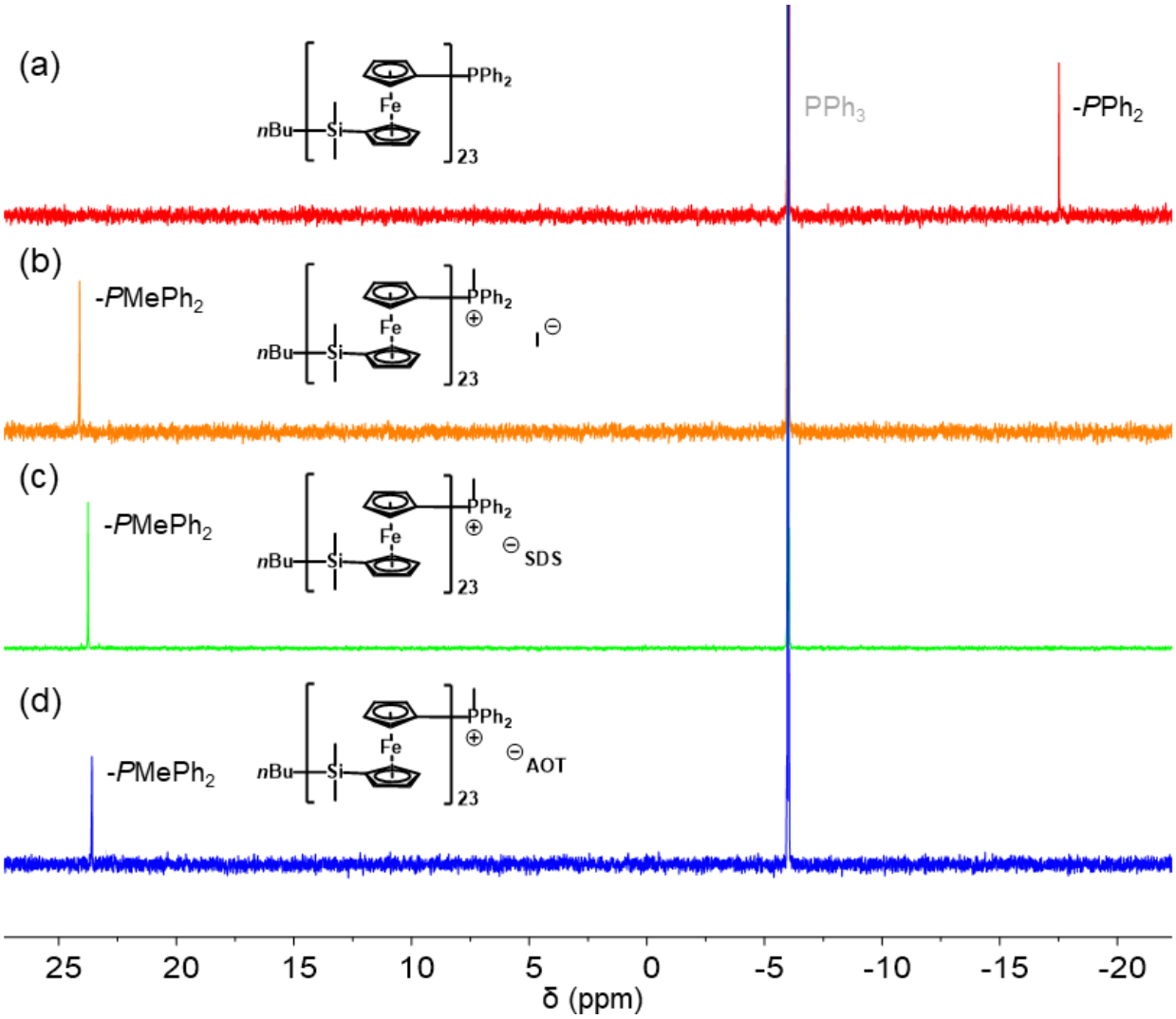

Fig. S2 ^{31}P NMR spectra of (a) $PFS_{23}PPh_2$ compared with quaternized (b) $PFS_{23}[PPh_2Me]I$, (c) $PFS_{23}[PPh_2Me]SDS$ and (d) $PFS_{23}[PPh_2Me]AOT$. Triphenylphosphine (100 mg/mL in THF) was used as an internal reference.

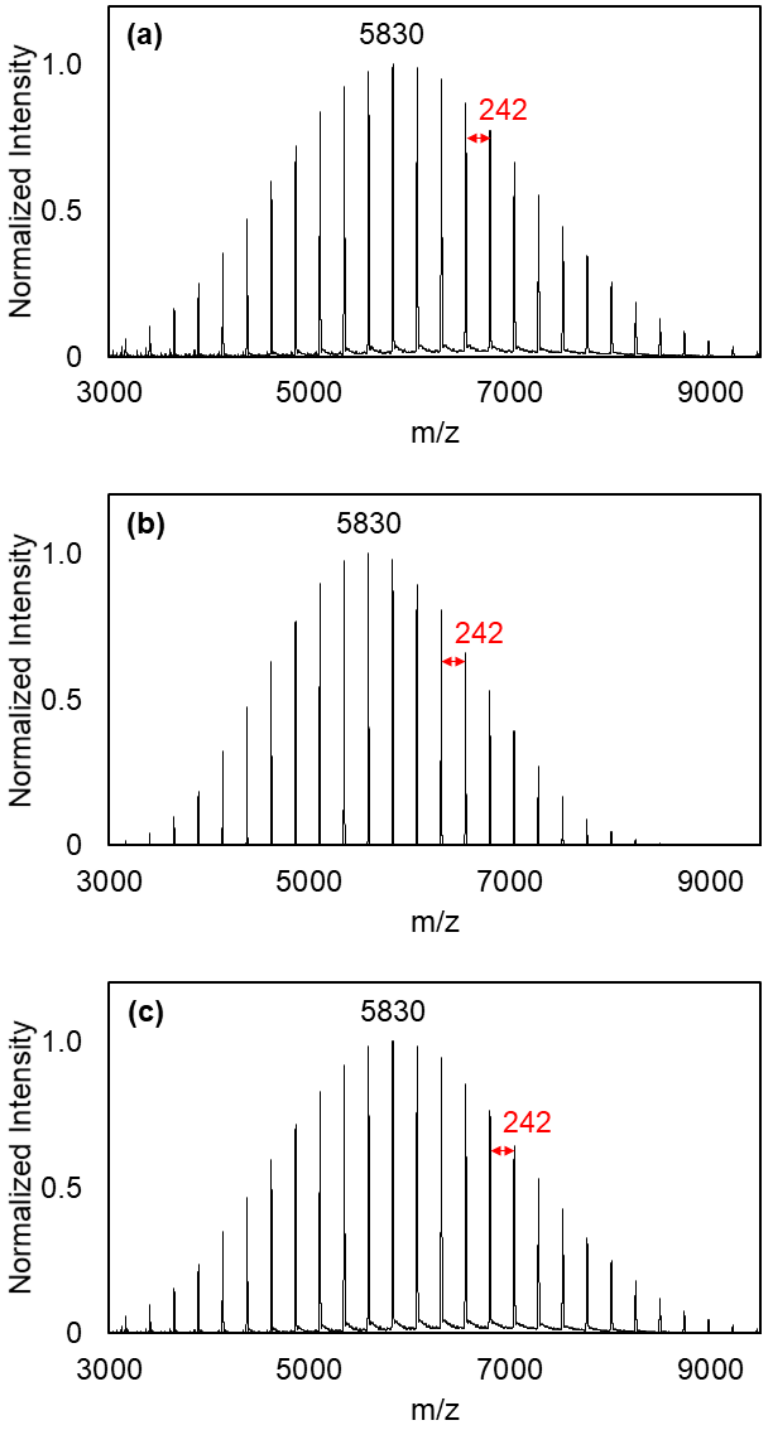

Fig S3 MALDI-TOF spectra of (a) $PFS_{23}[PPh_2Me]I$; $[M^+]$ = 5,830 Da, (b) $PFS_{23}[PPh_2Me]SDS$; $[M^+]$ = 5,830 Da and (c) $PFS_{23}[PPh_2Me]AOT$; $[M^+]$ = 5,830 Da. The mass difference between

each peak is equal to the molecular weight of a PFS monomer unit (242 Da). The spectra were obtained in positive mode, thus the counteranions cannot be observed.

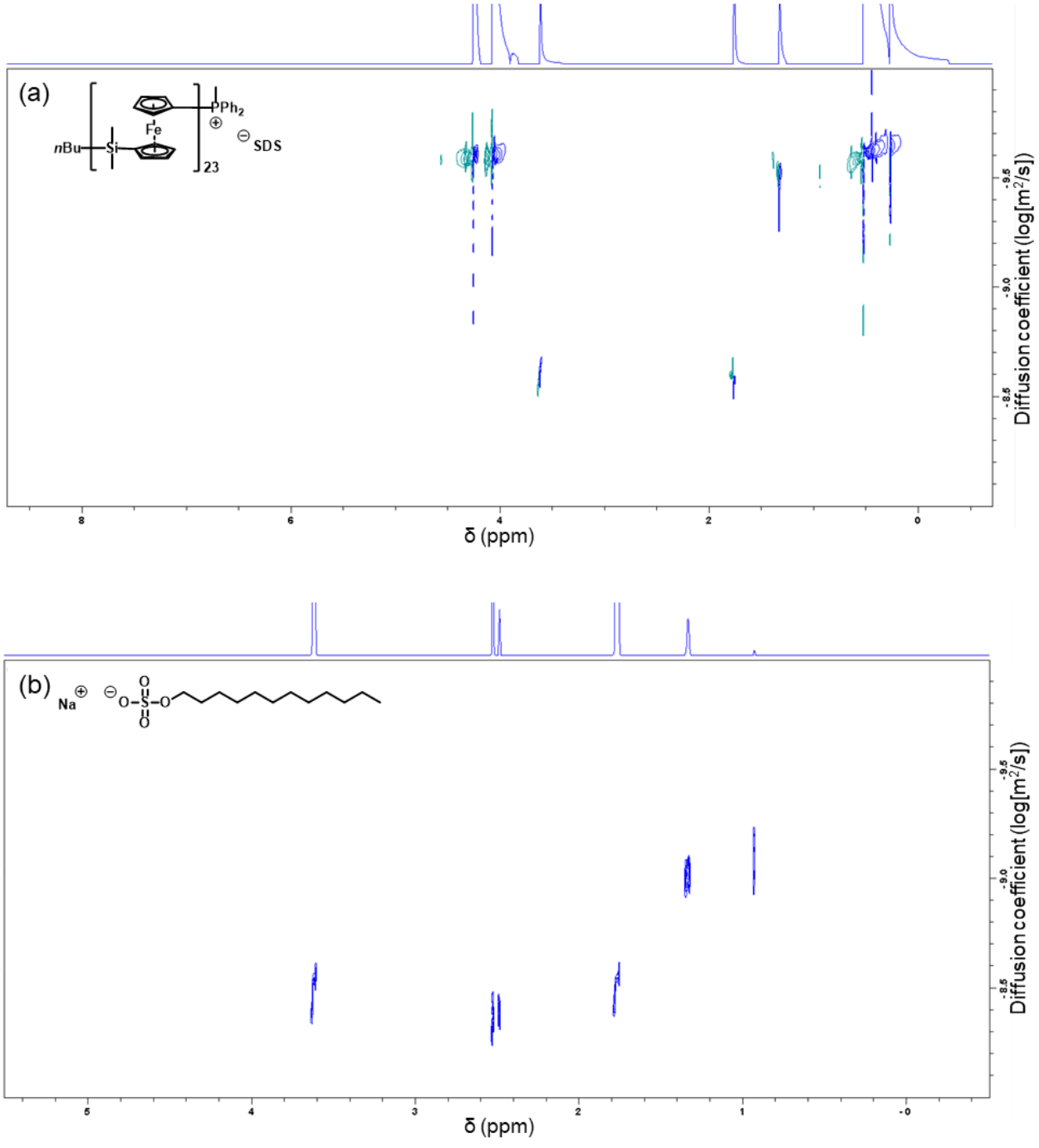

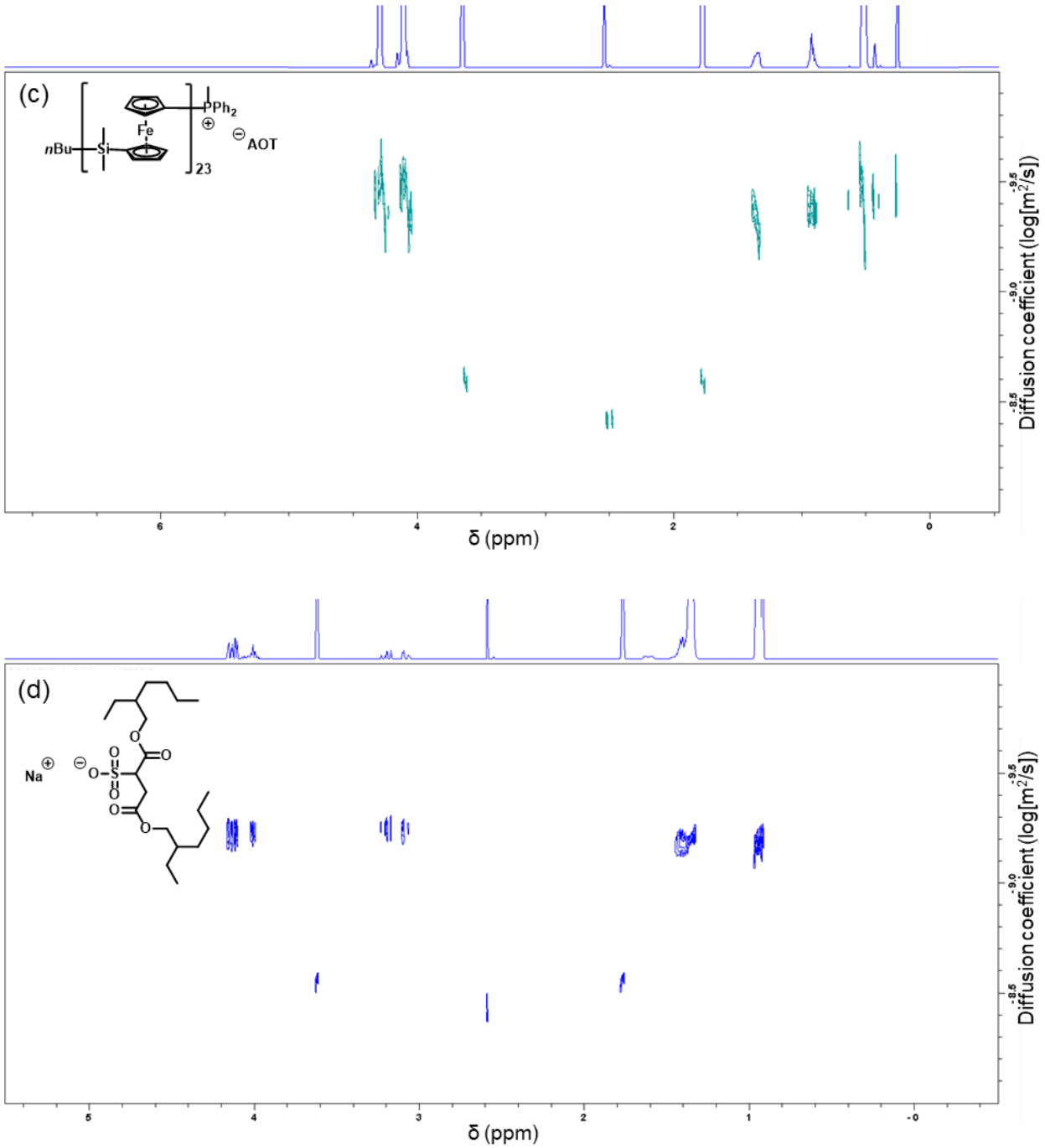

Fig. S4 ^{1}H DOSY NMR spectra of (a) $PFS_{23}[PPh_2Me]SDS$ and (c) $PFS_{23}[PPh_2Me]AOT$, compared with that of the sodium salts of the counteranions, (b) Na[SDS] and (d) Na[AOT]. All DOSY experiments were carried out in THF-d_8 at a concentration of ca. 5 mg/mL.

Supplementary Table S1 Diffusion coefficients of resonances arising from the surfactant counteranion obtained from ^{1}H DOSY NMR analysis of $PFS_{23}[PPh_2Me]X$ compared with that of the sodium salts of the counteranions, Na[SDS] and Na[AOT].

	δ (ppm)	Proton	Diffusion coefficient (m^2/s)
Na[SDS]	1.35–1.32	-C*H*$_2$-	4.94 x 10^{-5}
$PFS_{23}[PPh_2Me]$SDS	1.34–1.33		2.44 x 10^{-6}
Na[AOT]	0.96–0.91	-CH_2CH_3	4.47 x 10^{-9}
$PFS_{23}[PPh_2Me]$AOT	0.95–0.88		2.03 x 10^{-6}

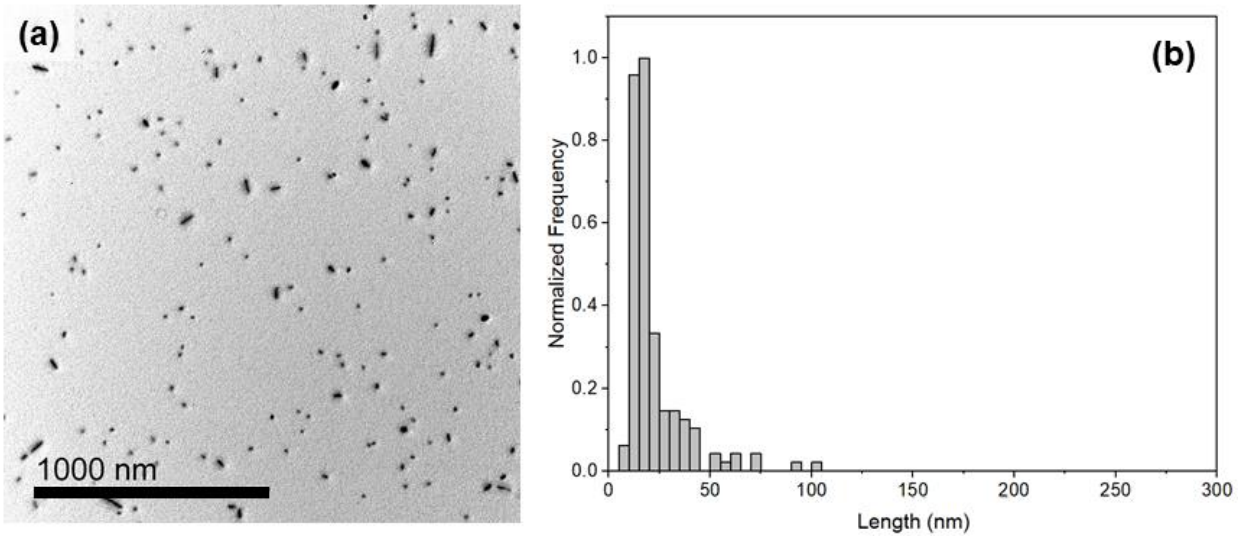

Fig. S5 (a) Representative TEM image of PFS_{24}-*b*-$P2VP_{384}$ 1D micelles prepared by sonication of polydisperse cylindrical micelles at 0 °C for 4 h. (b) Histogram of contour length distribution, L_n = 22 nm; L_w/L_n = 1.46; 5 mg/mL (0.6 wt%). Solution samples of 0.5 mg/mL were drop-cast and imaged after solvent evaporation. Scale bar = 1000 nm.

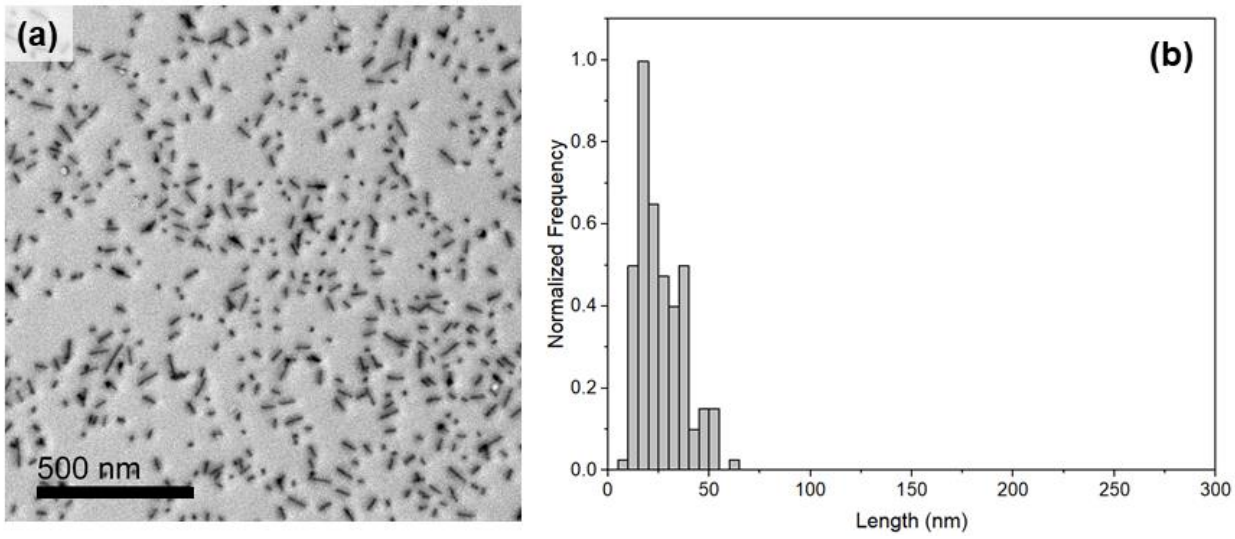

Fig. S6 (a) Representative TEM image of PFS_{24}-*b*-$P2VP_{384}$ 1D seed micelles used in this study. (b) Histogram of contour length distribution, L_n = 26 nm; L_w/L_n = 1.19; 5 mg/mL (0.6 wt%) in *i*PrOH. Solution samples of 1 mg/mL were drop-cast and imaged after solvent evaporation. Scale bar = 500 nm.

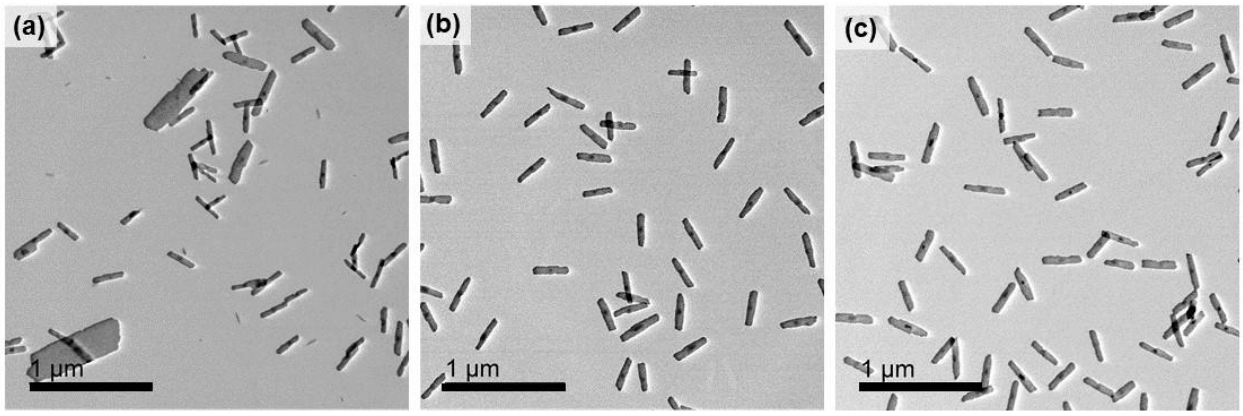

Fig. S7 Representative TEM images of PFS_{23}[PPh_2Me]SDS platelet micelles formed through seeded growth from PFS_{24}-*b*-$P2VP_{384}$ 1D micelles (L_n = 26 nm, L_w/L_n = 1.19) in *i*PrOH at 0.01 wt% and a m_{unimer}/m_{seed} of 10 prepared (a) in the absence of vigorous mixing (A_w/A_n = 3.44),

(b) with vigorous mixing for 3 s (as in this work) (A_w/A_n = 1.03), and (c) with a further 3 s of vigorous mixing (A_w/A_n = 1.03). Scale bar = 1000 nm.

Supplementary Table S2 Parameters obtained from statistical analysis of contour area measurements for $PFS_{23}[PPh_2Me]I$ platelet micelles formed through seeded growth from PFS_{24}-*b*-$P2VP_{384}$ 1D micelles (L_n = 26 nm, L_w/L_n = 1.19) in *i*PrOH at 0.01 wt% and various m_{unimer}/m_{seed}.

m_{unimer}/m_{seed}	A_n (x 10^2 nm^2)	σ (x 10^2 nm^2)	A_w/A_n	R_n	R_w/R_n
5	189	23	1.02	5.1	1.02
10	342	34	1.01	4.1	1.01
20	716	42	1.00	4.0	1.01
30	1086	85	1.01	3.9	1.00
40	1272	83	1.00	3.7	1.00

Supplementary Table S3 Parameters obtained from statistical analysis of contour area measurements for $PFS_{23}[PPh_2Me]SDS$ platelet micelles formed through seeded growth from PFS_{24}-*b*-$P2VP_{384}$ 1D micelles (L_n = 26 nm, L_w/L_n = 1.19) in *i*PrOH at 0.01 wt% and various m_{unimer}/m_{seed}.

m_{unimer}/m_{seed}	A_n (x 10^2 nm^2)	σ (x 10^2 nm^2)	A_w/A_n	R_n	R_w/R_n
5	173	21	1.01	4.7	1.02
10	320	56	1.03	5.1	1.02
20	633	63	1.01	4.0	1.01
30	952	88	1.01	3.5	1.01
40	1219	130	1.01	3.5	1.02

Supplementary Table S4 Parameters obtained from statistical analysis of contour area measurements for PFS_{23}[PPh_2Me]AOT platelet micelles formed through seeded growth from PFS_{24}-*b*-$P2VP_{384}$ 1D micelles (L_n = 26 nm, L_w/L_n = 1.19) in *i*PrOH at 0.01 wt% and various m_{unimer}/m_{seed}.

m_{unimer}/m_{seed}	A_n (x 10^2 nm^2)	σ (x 10^2 nm^2)	A_w/A_n	R_n	R_w/R_n
5	289	32	1.01	3.8	1.01
10	319	29	1.01	3.5	1.01
20	702	82	1.01	3.0	1.01
30	829	65	1.01	3.3	1.01
40	1373	123	1.01	2.7	1.00

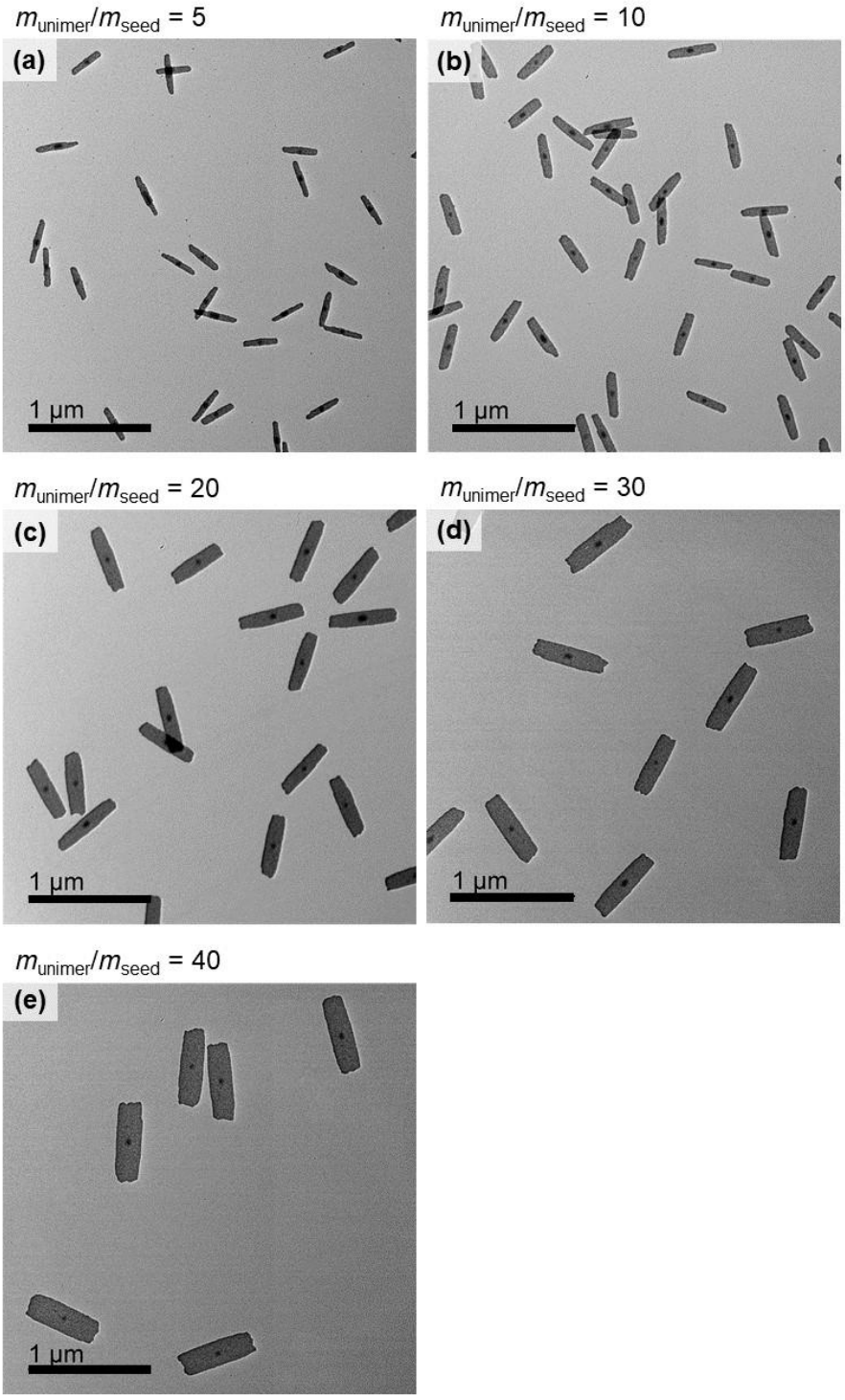

Fig. S8 Representative TEM images of $PFS_{23}[PPh_2Me]I$ platelet micelles formed through seeded growth from PFS_{24}-*b*-$P2VP_{384}$ 1D micelles (L_n = 26 nm, L_w/L_n = 1.19) in *i*PrOH at 0.1 mg/mL (0.01 wt%) and various m_{unimer}/m_{seed}. Scale bar = 1000 nm.

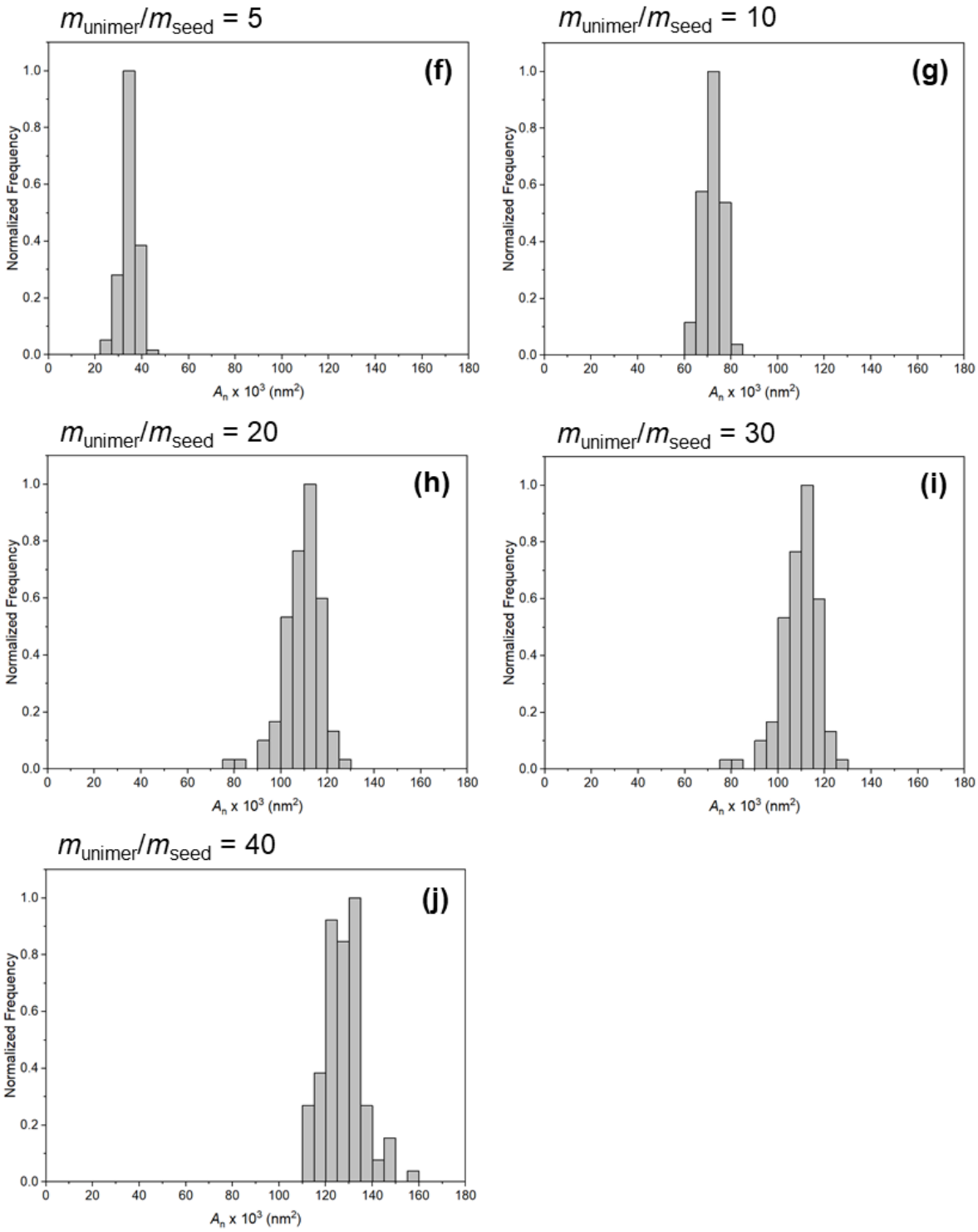

Fig. S9 Contour area distributions of PFS_{23}[PPh_2Me]I platelet micelles formed through seeded growth from PFS_{24}-*b*-$P2VP_{384}$ 1D micelles (L_n = 26 nm, L_w/L_n = 1.19) in *i*PrOH at 0.1 mg/mL (0.01 wt%) and various m_{unimer}/m_{seed}.

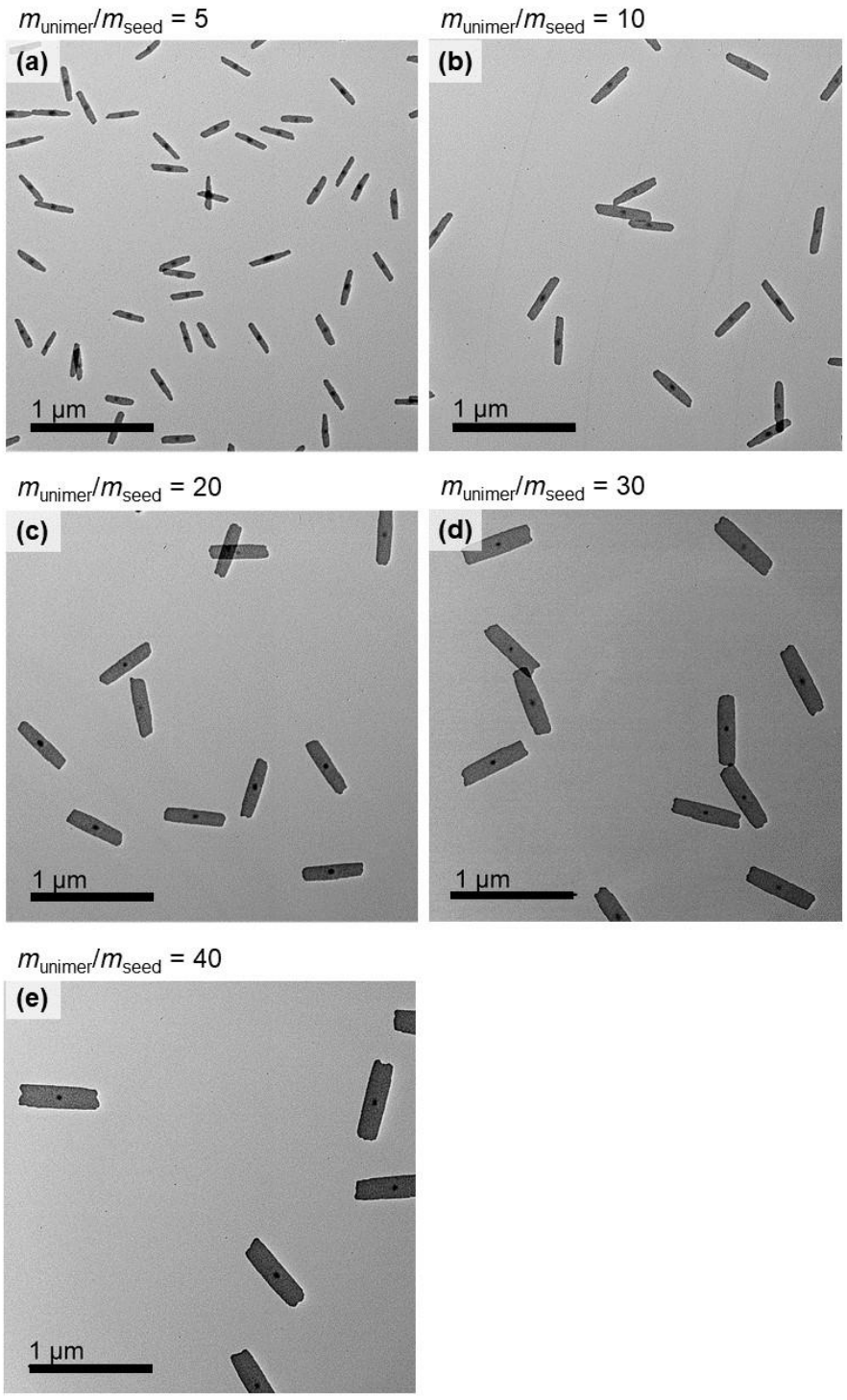

Fig. S10 Representative TEM images of PFS_{23}[PPh_2Me]SDS platelet micelles formed through seeded growth from PFS_{24}-*b*-$P2VP_{384}$ 1D micelles (L_n = 26 nm, L_w/L_n = 1.19) in *i*PrOH at 0.1 mg/mL (0.01 wt%) and various m_{unimer}/m_{seed}. Scale bar = 1000 nm.

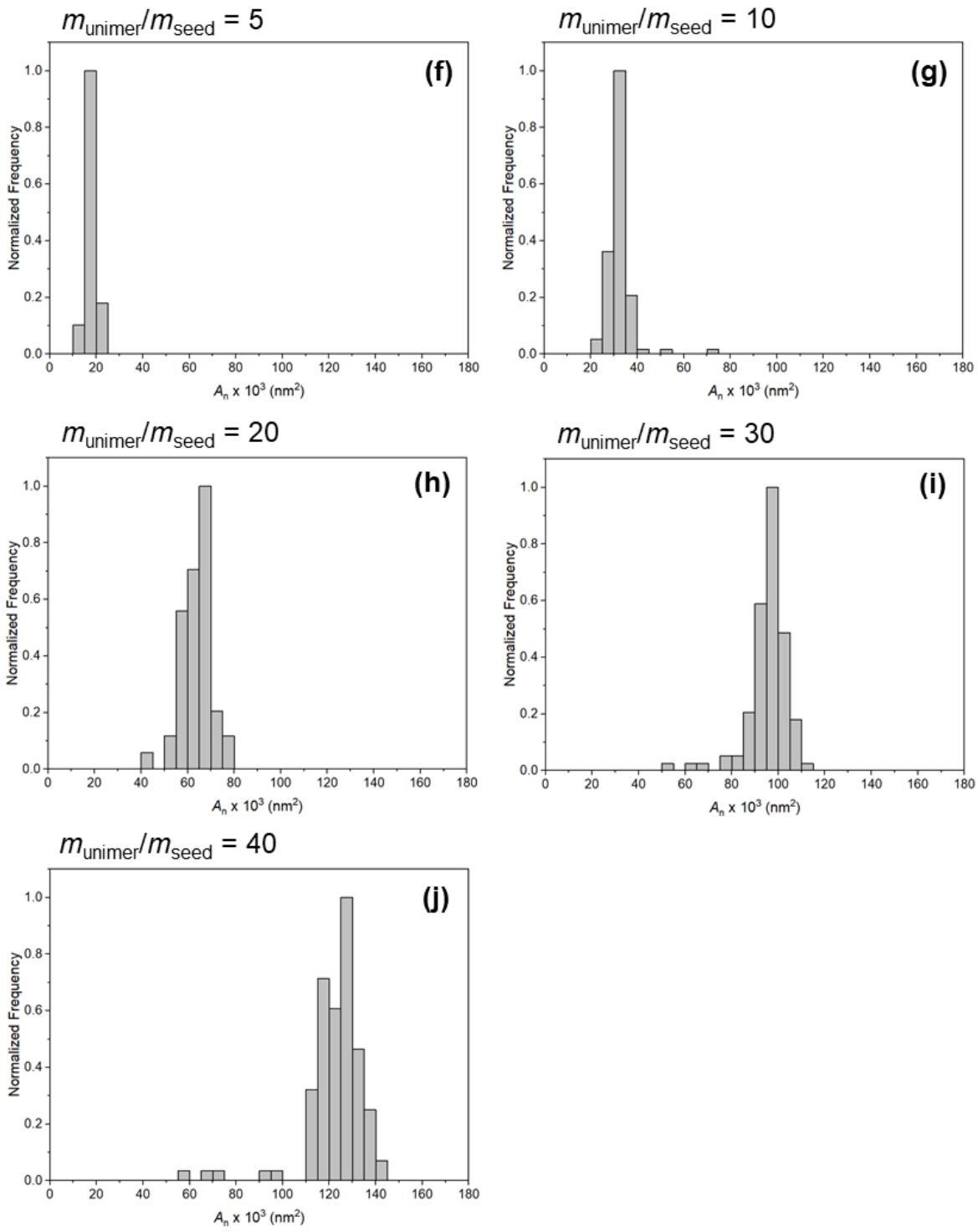

Fig. S11 Contour area distributions of PFS_{23}[PPh_2Me]SDS platelet micelles formed through seeded growth from PFS_{24}-*b*-$P2VP_{384}$ 1D micelles (L_n = 26 nm, L_w/L_n = 1.19) in *i*PrOH at 0.1 mg/mL (0.01 wt%) and various m_{unimer}/m_{seed}.

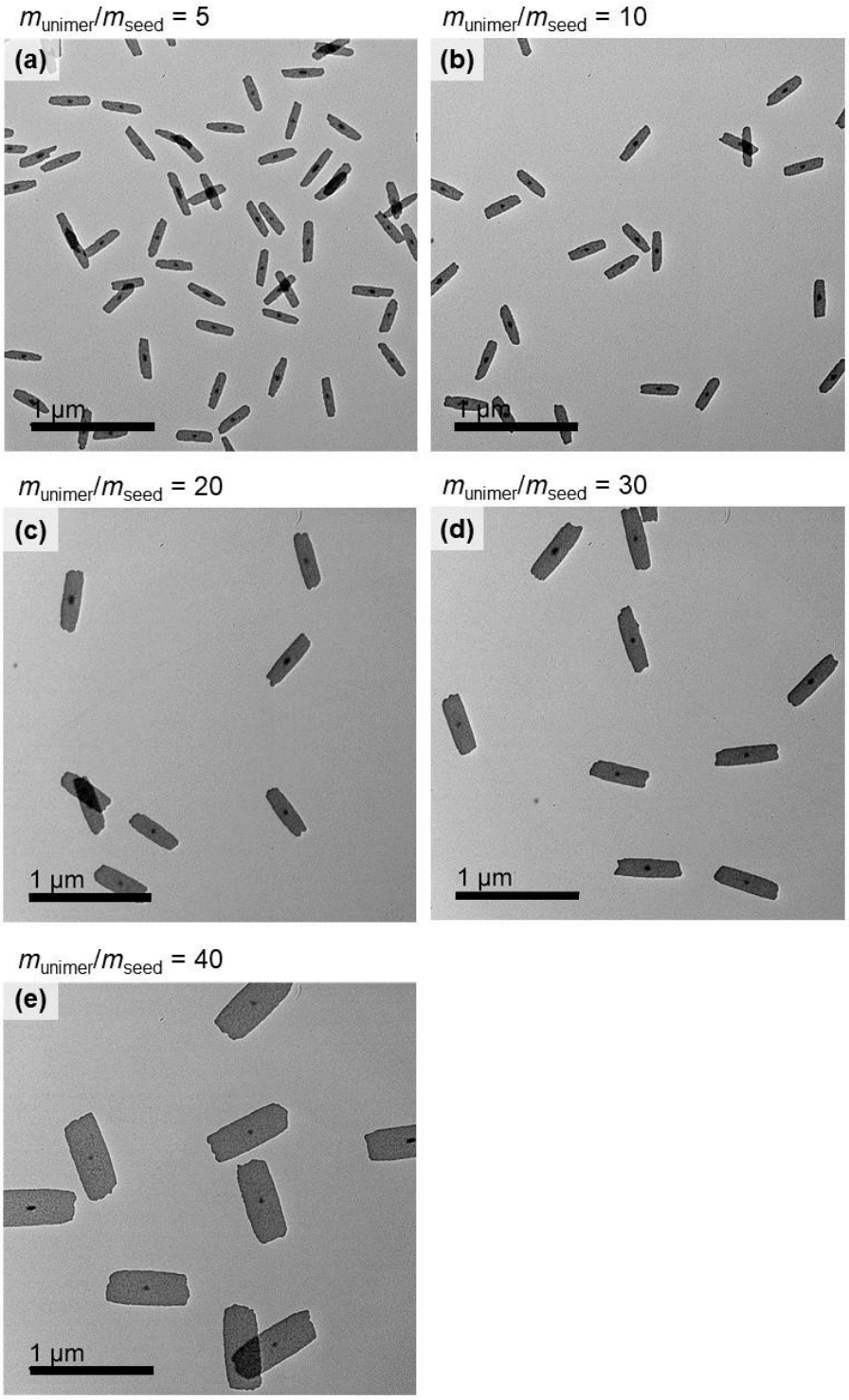

Fig. S12 Representative TEM images of PFS_{23}[PPh_2Me]AOT platelet micelles formed through seeded growth from PFS_{24}-*b*-$P2VP_{384}$ 1D micelles (L_n = 26 nm, L_w/L_n = 1.19) in *i*PrOH at 0.1 mg/mL (0.01 wt%) and various m_{unimer}/m_{seed}. Scale bar = 1000 nm.

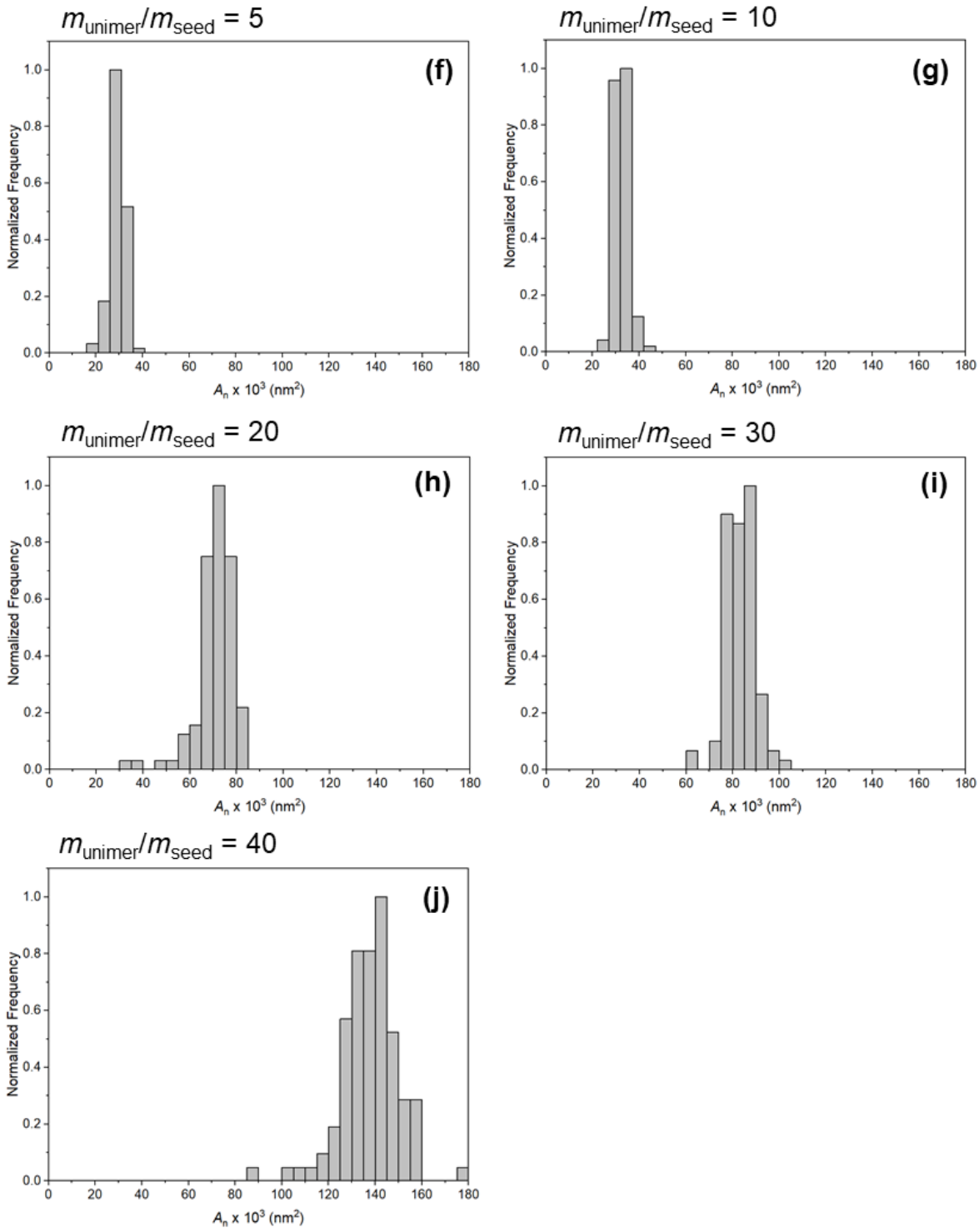

Fig. S13 Contour area distributions of PFS_{23}[PPh_2Me]AOT platelet micelles formed through seeded growth from PFS_{24}-*b*-$P2VP_{384}$ 1D micelles (L_n = 26 nm, L_w/L_n = 1.19) in *i*PrOH at 0.1 mg/mL (0.01 wt%) and various m_{unimer}/m_{seed}.

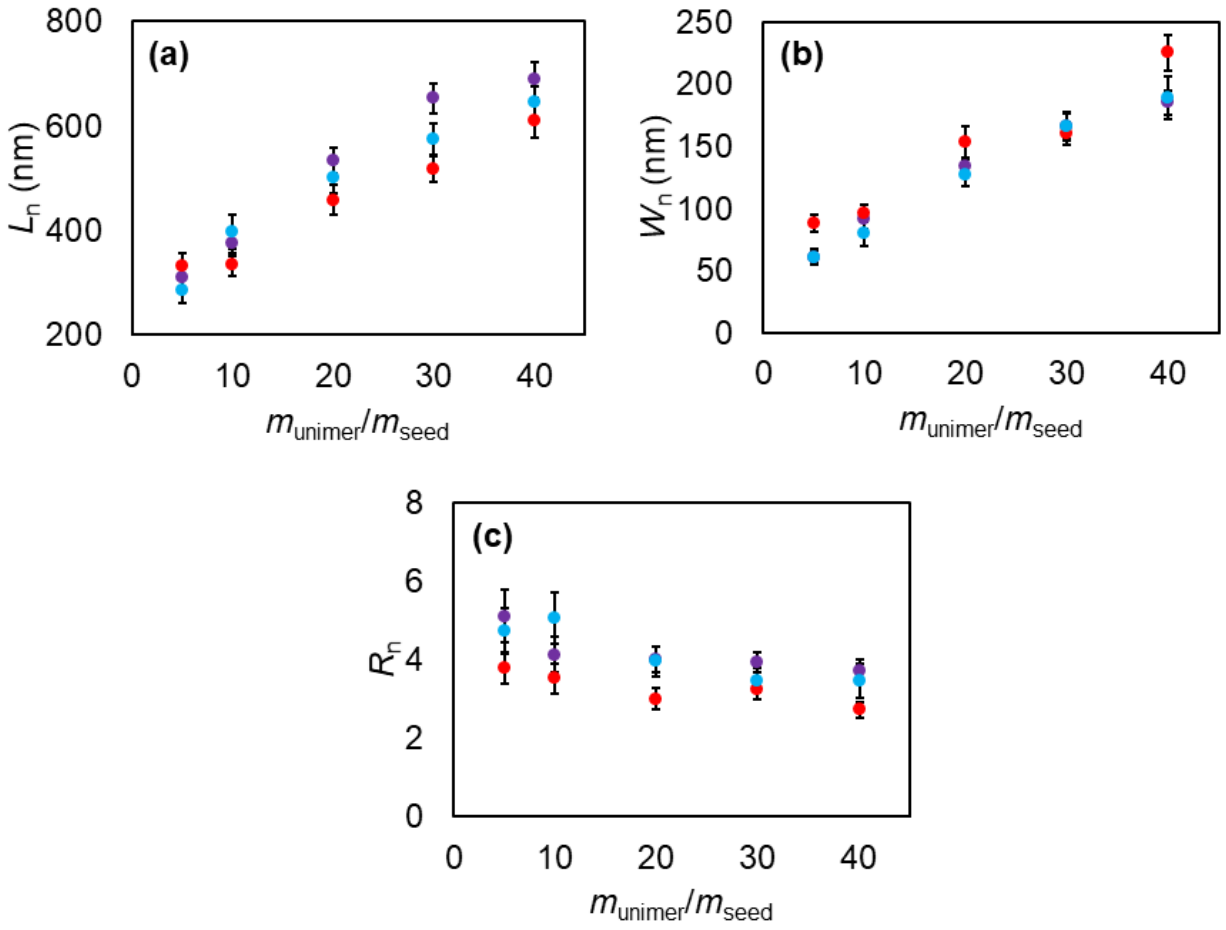

Fig. S14 Dependence of $PFS_{23}[PPh_2Me]X$ platelet (a) number-average length (L_n), (b) number-average width (W_n) and (c) number-average aspect ratio (R_n) on m_{unimer}/m_{seed} in *i*PrOH at 0.01 wt%. X = I (purple), SDS (blue), AOT (red). Error bars represent the standard deviation of measured lengths, widths, or areas.

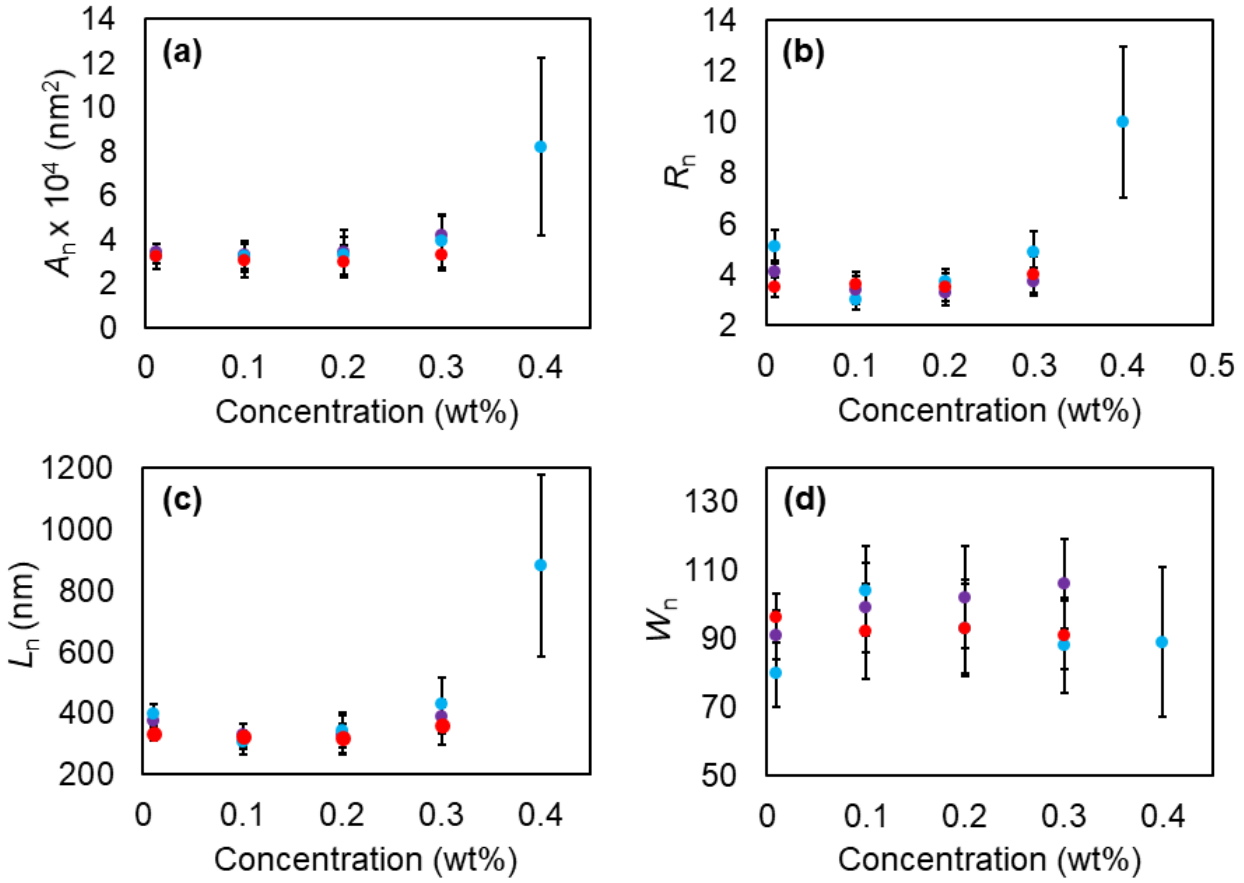

Fig. S15 Dependence of $PFS_{23}[PPh_2Me]X$ platelet (a) number-average area (A_n), (b) number-average aspect ratio (R_n), (c) number-average length (L_n), and (d) number-average width (W_n) on 2D living CDSA concentration in *i*PrOH. X = I (purple), SDS (blue), AOT (red). Error bars represent the standard deviation of measured areas, lengths and widths, or calculated aspect ratios.

Supplementary Table S5 Parameters obtained from statistical analysis of contour area measurements for $PFS_{23}[PPh_2Me]I$ platelet micelles formed through seeded growth from PFS_{24}-*b*-$P2VP_{384}$ 1D micelles (L_n = 26 nm, L_w/L_n = 1.19) in *i*PrOH. All experiments were carried out at room temperature (22 ºC) and a m_{unimer}/m_{seed} of 10.

wt%	A_n (x 10^2 nm^2)	σ (x 10^2 nm^2)	A_w/A_n	R_n	R_w/R_n
0.01	342	34	1.01	4.1	1.01
0.1	327	63	1.04	3.4	1.02
0.2	342	102	1.09	3.3	1.02
0.3	415	98	1.06	3.7	1.02
0.4	-	-	-	-	-

Supplementary Table S6 Parameters obtained from statistical analysis of contour area measurements for $PFS_{23}[PPh_2Me]SDS$ platelet micelles formed through seeded growth from PFS_{24}-*b*-$P2VP_{384}$ 1D micelles (L_n = 26 nm, L_w/L_n = 1.19) in *i*PrOH. All experiments were carried out at room temperature (22 ºC) and a m_{unimer}/m_{seed} of 10.

wt%	A_n (x 10^2 nm^2)	σ (x 10^2 nm^2)	A_w/A_n	R_n	R_w/R_n
0.01	320	56	1.03	5.1	1.02
0.1	321	69	1.05	3.0	1.02
0.2	325	87	1.07	3.7	1.02
0.3	389	115	1.09	4.9	1.03
0.4	821	400	1.24	10.0	1.09

Supplementary Table S7 Parameters obtained from statistical analysis of contour area measurements for PFS_{23}[PPh_2Me]AOT platelet micelles formed through seeded growth from PFS_{24}-*b*-$P2VP_{384}$ 1D micelles (L_n = 26 nm, L_w/L_n = 1.19) in *i*PrOH. All experiments were carried out at room temperature (22 ºC) and a m_{unimer}/m_{seed} of 10.

wt%	A_n (x 10^2 nm^2)	σ (x 10^2 nm^2)	A_w/A_n	R_n	R_w/R_n
0.01	319	32	1.01	3.5	1.01
0.1	303	73	1.06	3.6	1.02
0.2	300	75	1.06	3.5	1.02
0.3	330	74	1.05	4.0	1.03
0.4	-	-	-	-	-

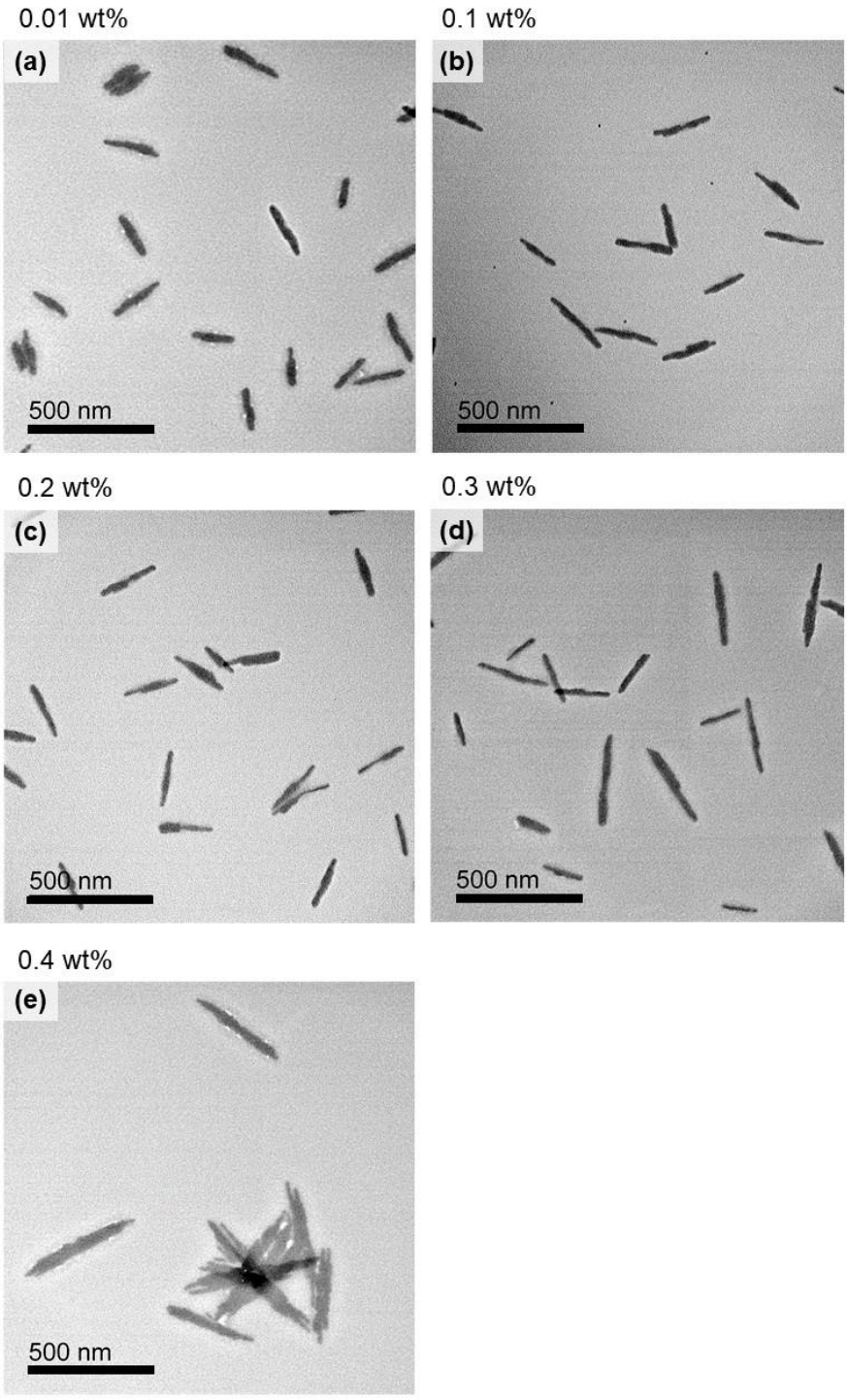

Fig. S16 Representative TEM image of lenticular-like platelets from seeded growth of PFS_{20}-*b*-$P2VP_{19}$ from PFS_{24}-*b*-$P2VP_{384}$ 1D micelles (L_n = 26 nm, L_w/L_n = 1.19) in *i*PrOH at (a) 0.01 wt%, (b) 0.1 wt%, (c) 0.2 wt%, (d) 0.3 wt%, and (e) 0.4 wt%. Scale bar = 500 nm.

Supplementary Table S8 Parameters obtained from statistical analysis of contour area measurements for PFS_{20}-*b*-$P2VP_{19}$ platelet micelles formed through seeded growth from PFS_{24}-*b*-$P2VP_{384}$ 1D micelles (L_n = 26 nm, L_w/L_n = 1.19) in *i*PrOH. All experiments were carried out at room temperature (22 ºC) and a m_{unimer}/m_{seed} of 10.

wt%	A_n (x 10^2 nm^2)	σ (x 10^2 nm^2)	A_w/A_n	R_n	R_w/R_n
0.01	84	19	1.05	4.6	1.04
0.1	94	24	1.07	5.8	1.05
0.2	81	27	1.11	6.2	1.07
0.3	84	38	1.20	6.4	1.08
0.4	197	70	1.13	6.8	1.05

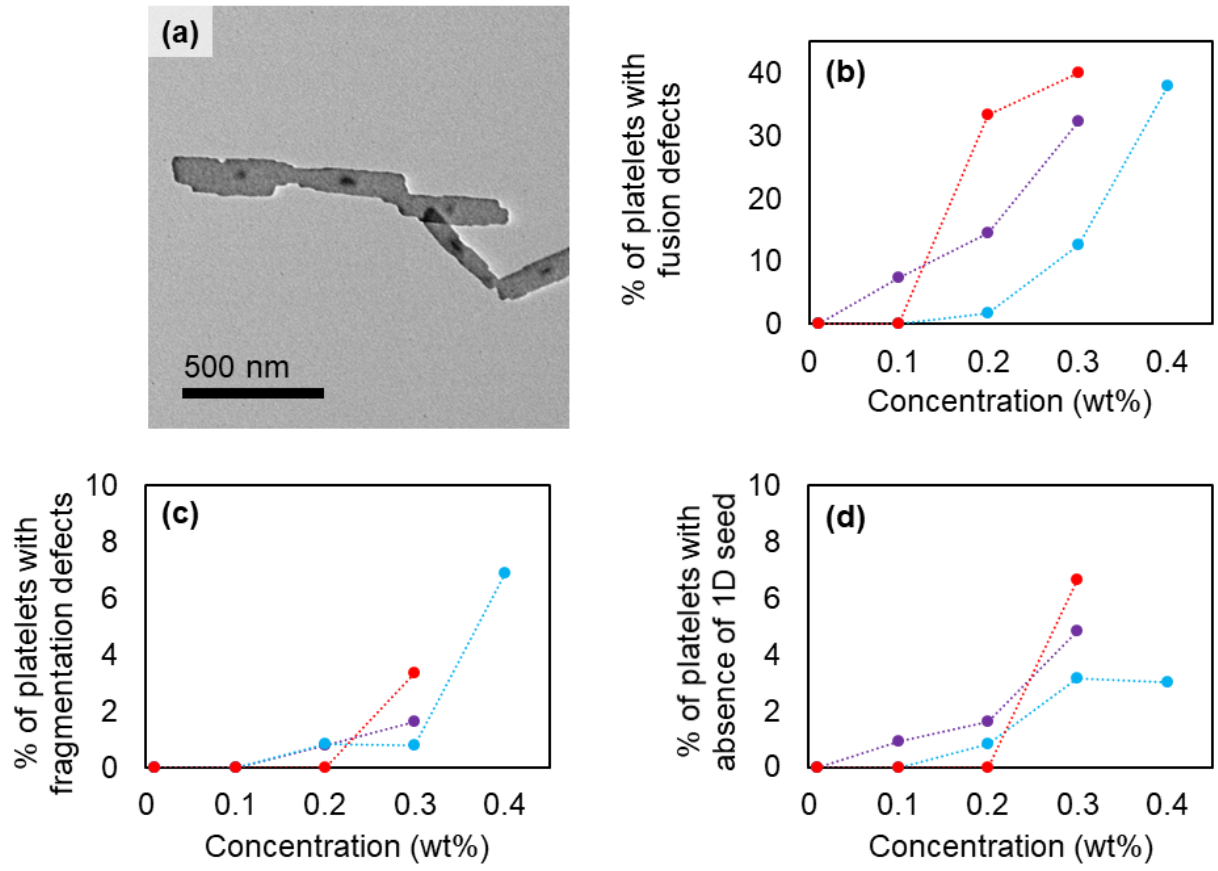

Fig. S17 (a) Representative TEM image of platelet fusion defects observed in 2D living CDSA at higher concentrations (0.1–0.4 wt%). This example is taken from the living CDSA of $PFS_{23}[PPh_2Me]I$ at a m_{unimer}/m_{seed} of 10, carried out at 0.3 wt% *i*PrOH. It shows a "trimer" and "dimer", both formed through fusion defects. This is contrary to nanostructure overlap, which can be observed as the area of higher electron contrast where the "trimer" and "dimer" have physically aggregated, presumably on solvent evaporation during TEM sample preparation. Dependence of the percentage of $PFS_{23}[PPh_2Me]X$ platelets with (b) fusion defects, (c) fragmentation defects, or (d) in the absence of a 1D seed on the 2D living CDSA concentration. X = I (purple), SDS (blue), AOT (red). Trend lines for guidance only.

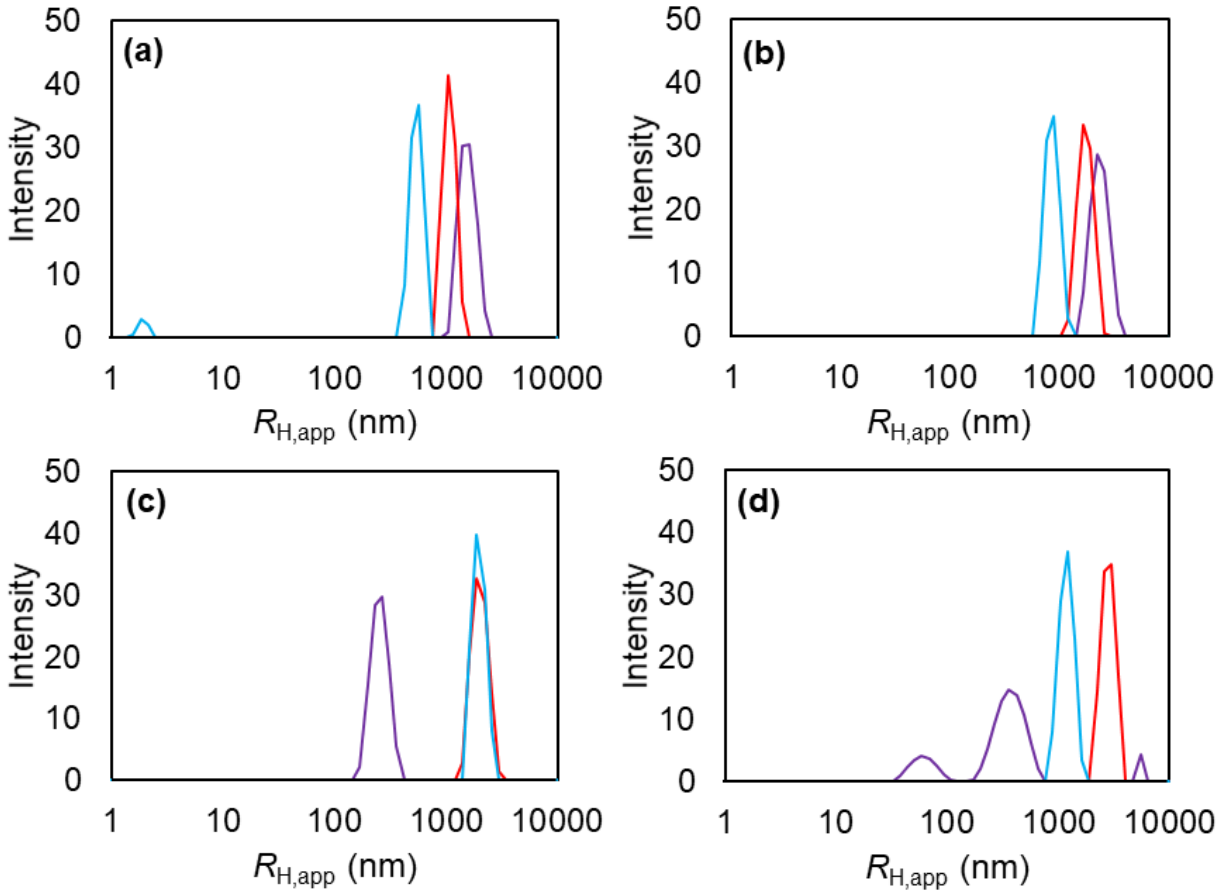

Fig. S18 Representative intensity distribution DLS plots of $PFS_{23}[PPh_2Me]X$ platelet micelles formed through seeded growth from PFS_{24}-*b*-$P2VP_{384}$ 1D micelles (L_n = 26 nm, L_w/L_n = 1.19) in *i*PrOH at a m_{unimer}/m_{seed} of 10 and at (a) 0.1 wt%, (b) 0.2 wt%, (c) 0.3 wt%, and (d) 0.4 wt%. X = I (purple), SDS (blue), AOT (red).

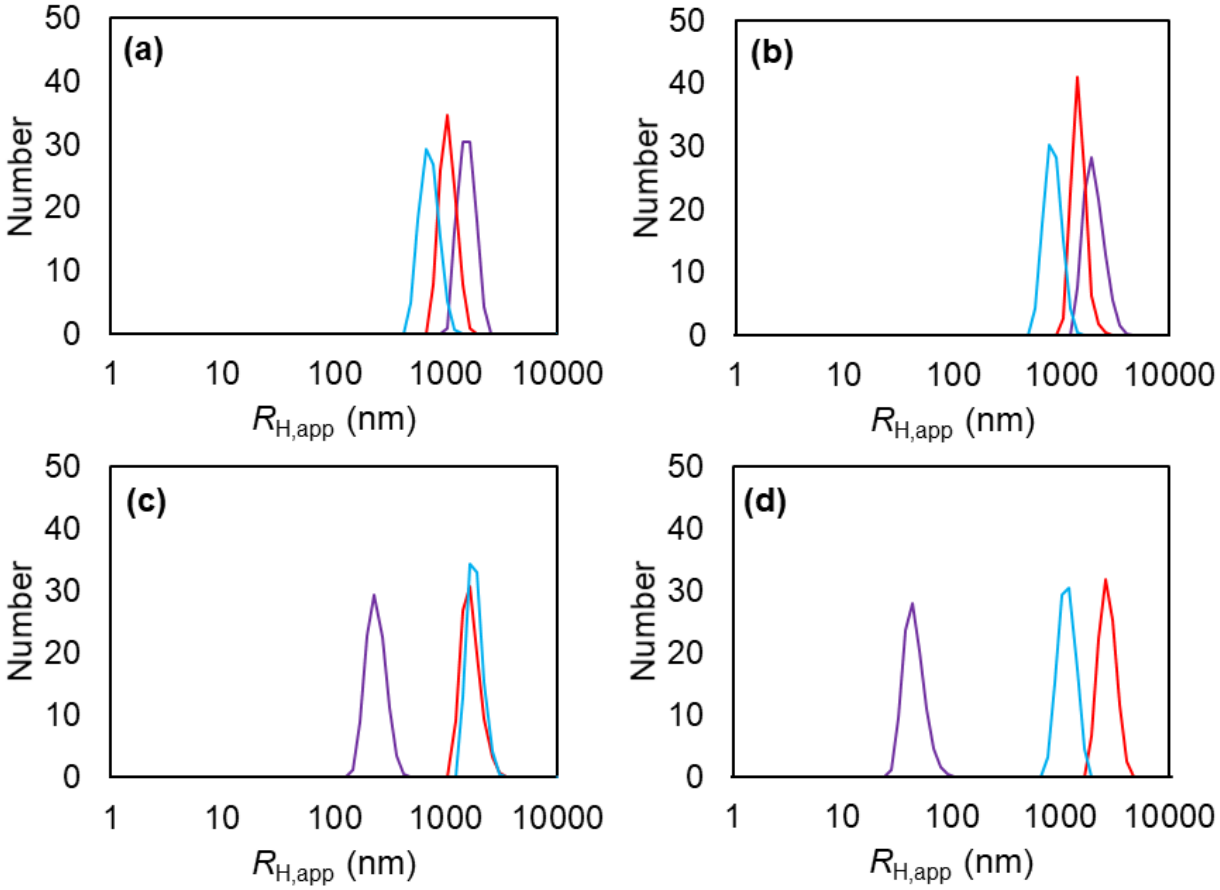

Fig. S19 Representative number distribution DLS plots of $PFS_{23}[PPh_2Me]X$ platelet micelles formed through seeded growth from PFS_{24}-*b*-$P2VP_{384}$ 1D micelles (L_n = 26 nm, L_w/L_n = 1.19) in *i*PrOH at a m_{unimer}/m_{seed} of 10 and at (a) 0.1 wt%, (b) 0.2 wt%, (c) 0.3 wt%, and (d) 0.4 wt%. X = I (purple), SDS (blue), AOT (red).

Supplementary Table S9 Average apparent hydrodynamic radii ($R_{H,app}$) for $PFS_{23}[PPh_2Me]X$ platelet micelles formed through seeded growth from PFS_{24}-*b*-$P2VP_{384}$ 1D micelles (L_n = 26 nm, L_w/L_n = 1.19) in *i*PrOH. All self-assembly experiments were carried out at room temperature (22 ºC) and a m_{unimer}/m_{seed} of 10. Values are calculated from five repeat scattering experiments.

	$PFS_{23}[PPh_2Me]I$		$PFS_{23}[PPh_2Me]SDS$		$PFS_{23}[PPh_2Me]AOT$	
wt%	$R_{H,app}$ (nm)	σ (nm)	$R_{H,app}$ (nm)	σ (nm)	$R_{H,app}$ (nm)	σ (nm)
0.1	2127	743	2312	600	3274	432
0.2	2233	340	2390	634	2229	396
0.3	1162	417	3991	939	2618	158
0.4	270	160	1081	57	2314	273

Supplementary Table S10 Number-average length (L_n) (obtained from statistical analysis of contour length) for $PFS_{23}[PPh_2Me]X$ platelet micelles formed through seeded growth from PFS_{24}-*b*-$P2VP_{384}$ 1D micelles (L_n = 26 nm, L_w/L_n = 1.19) in *i*PrOH. All self-assembly experiments were carried out at room temperature (22 ºC) and a m_{unimer}/m_{seed} of 10.

	$PFS_{23}[PPh_2Me]I$		$PFS_{23}[PPh_2Me]SDS$		$PFS_{23}[PPh_2Me]AOT$	
wt%	L_n (nm)	σ (nm)	L_n (nm)	σ (nm)	L_n (nm)	σ (nm)
0.1	330	38	306	39	326	41
0.2	330	63	345	56	319	48
0.3	387	55	432	85	360	60
0.4	-	-	881	297	-	-

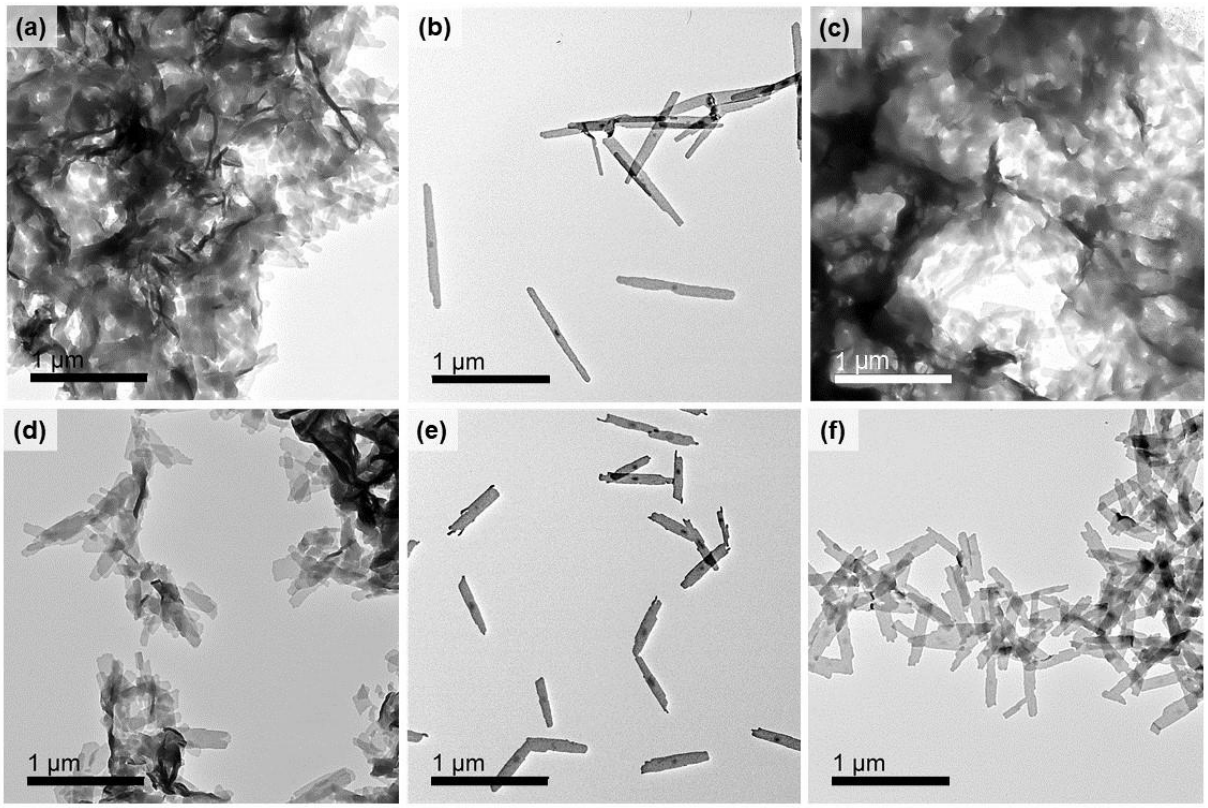

Fig. S20 Representative TEM images of (a), (d) $PFS_{23}[PPh_2Me]I$, (b), (e) $PFS_{23}[PPh_2Me]SDS$ and (c), (f) $PFS_{23}[PPh_2Me]AOT$ platelet micelles formed through high concentration (0.4 wt%) seeded growth at (a)–(c) 22 ºC or (d)–(f) 40 ºC from PFS_{24}-*b*-$P2VP_{384}$ 1D micelles (L_n = 26 nm, L_w/L_n = 1.19) in *i*PrOH at m_{unimer}/m_{seed} = 10. Scale bar = 1000 nm.

Supplementary Table S11 Parameters obtained from statistical analysis of contour area measurements for $PFS_{23}[PPh_2Me]X$ platelet micelles formed through seeded growth from PFS_{24}-*b*-$P2VP_{384}$ 1D micelles (L_n = 26 nm, L_w/L_n = 1.19) in *i*PrOH. Experiments were carried out at 40 °C and a m_{unimer}/m_{seed} of 10.

Homopolymer	A_n (x 10^2 nm^2)	σ (x 10^2 nm^2)	A_w/A_n	R_n	R_w/R_n
$PFS_{23}[PPh_2Me]I$	-	-	-	-	-
$PFS_{23}[PPh_2Me]SDS$	554	188	1.12	4.6	1.02
$PFS_{23}[PPh_2Me]AOT$	543	168	1.10	4.5	1.03

References

1 D. A. Rider, K. A. Cavicchi, K. N. Power-Billard, T. P. Russell and I. Manners, *Macromolecules*, 2005, **38**, 6931–6938.

2 X. He, M.-S. Hsiao, C. E. Boott, R. L. Harniman, A. Nazemi, X. Li, M. A. Winnik and I. Manners, *Nat. Mater.*, 2017, **16**, 481–488.

3 H. Wang, M. A. Winnik and I. Manners, *Macromolecules*, 2007, **40**, 3784–3789.